Quantum multimode treatment of light scattering by an atom in a waveguide

William Konyk and Julio Gea-Banacloche
Department of Physics, University of Arkansas, Fayetteville, Arkansas 72701, USA
(Received 4 February 2016; published 8 June 2016)

We present a full multimode treatment of the interaction of the quantized radiation field with a single two-level atom in a one-dimensional waveguide configuration. Starting with an incident pulse consisting of an arbitrary (finite) number of photons in a general initial state, we derive the equations of motion and a closed-form expression for the shape of the pulse after its interaction with the atom. We then specialize our results to the two-photon case where a number of analytical results can be derived, for both unidirectional and bidirectional systems. We study the effects of different pulse shapes, the manifestations of the entangled, so-called bound state of the two photons, single- and two-photon detection probabilities, and provide simple approximate results for the strong-coupling (or adiabatic, or long-pulse) regime. We also discuss the requirements for a true unidirectional setup, and the application of such a setup to photon sorting proposed by Witthaut, Lukin, and Sørensen [Europhys. Lett. **97**, 50007 (2012)].

DOI: 10.1103/PhysRevA.93.063807

I. INTRODUCTION AND SUMMARY

The development of single-photon sources, particularly for use in quantum information processing, has led to an interest in the study of the interaction of Fock-state wave packets with atoms, often in constrained geometries such as one-dimensional (1D) waveguides. Several groups have, in recent years, approached this problem from a variety of perspectives, such as S-matrix [1], scattering eigenstates [2,3], input-output methods [4], Green's functions [5], Langevin equations of motion [6], or direct integration of the Heisenberg [7,8] or Schrödinger equations [9–12]. Possible applications have been discussed, for instance, in Ref. [13].

In this paper we focus on the interaction of a Fock-state wave packet with a single two-level atom, and show that, in the absence of losses (that is, provided the evolution is unitary) the time-dependent Schrödinger equation can in principle be directly solved to yield analytical expressions for the scattered photon wave packets in real space, for incident wave packets of arbitrary shape, correlation or photon number N. Our formalism is a simple extension of the multimode description of nonclassical fields introduced in Ref. [14]. It yields expressions that can be directly used to compute, for traveling wave fields, the effective N-photon wave functions from which one can derive the N-photon detection probabilities, and a number of other quantities of interest (including the pulse spectrum, if desired). For quantum information applications, our results could also be used directly to calculate the fidelity of the final state to a desired reference state.

The outline of this paper is as follows. In Sec. II we show how the Schrödinger equations of motion for a quantized pulse interacting with a two-level atom in a one-dimensional configuration can be formally solved exactly, for a pulse containing a finite number of photons N. We relate the solution to the concept of effective N-photon wave functions, and provide several examples of the general solutions for different types of initial states, including explicitly up to three photons.

In Sec. III, we show how the results generalize to a bidirectional waveguide, and we study in depth the $N = 2$ case. Here, a large number of previous results are available, and we have noted the correspondence with earlier works in the references where appropriate. Like most of these works, we consider explicitly the case of Gaussian pulses, but we also extend our study to consider initial flat-top pulses, which are a smooth variant of the square pulses also found in other works (such as Refs. [8,9]). We cover both the case when the pulses come from the same direction [2] and the case when they are incident from opposite ends of the waveguide, where we make the connection with the corresponding recent results of Roulet *et al.* [8]. We look in detail at the shape of the scattered pulses in all these cases, through an explicit consideration of the corresponding one- and two-photon detection probabilities, discuss the entangled component of the state at length, and obtain simple analytical expressions that explain many of the features seen in the adiabatic (long-pulse, or large-coupling) limit.

Additional results are found in the Appendices. In Appendix A, we provide the results for our two-photon wave functions in the frequency domain (that is to say, the pulse spectra), for easier comparison with previous results. In Appendix B, we discuss briefly the applicability of the unidirectional waveguide formalism to real-world experimental setups, in particular in the context of an interesting scheme proposed by Witthaut *et al.* [13].

II. TWO-LEVEL ATOM INTERACTING WITH A QUANTIZED PULSE IN ONE DIMENSION

A. Solving the Schrödinger equations of motion for an N-photon state

We start by considering the interaction of a single two-level atom with a single set of modes, described in the interaction picture and at the location of the atom by the operator

$$A(t) = \frac{1}{\sqrt{2\pi}} \int_{-\infty}^{\infty} d\omega e^{-i\omega t} a_\omega, \tag{1}$$

where the a_ω are single-mode annihilation operators in the continuum formalism, satisfying $[a_\omega, a^\dagger_{\omega'}] = \delta(\omega - \omega')$, from which it follows that $[A(t), A^\dagger(t')] = \delta(t - t')$. The atom-field interaction Hamiltonian can then be written as

$$H = -i\hbar g[\sigma_+ A(t) - \sigma_- A^\dagger(t)], \tag{2}$$

where we define $\sigma_\pm$ to be the raising and lowering operators of the atom and g is a coupling constant that we assume to be frequency independent over the relatively narrow bandwidth of the incident field. If the operators a_ω represent traveling-wave modes, the Hamiltonian (2) describes the somewhat unintuitive case of a one-sided waveguide (but see Appendix B below for possible approximate realizations); however, as we shall show later, the exact same form can also be used to describe a two-sided waveguide if the operators a_ω are taken to represent standing-wave modes, so at this point there is no loss of generality.

Note also that we have defined ω as a frequency relative to the atomic transition, so that when $\omega = 0$ the light is in resonance with the atom. Then, with a symmetric incident field spectrum, the Hamiltonian (2) describes an essentially resonant interaction. To deal with a significantly detuned field (which will not be considered in this paper), explicit detuning terms $e^{\pm i\Delta t}$ could be added to (2).

As the atom is assumed to be a two-level atom, the total system state, at any given time, can be written as $|\psi\rangle = |\psi_e\rangle|e\rangle + |\psi_g\rangle|g\rangle$, where $|e\rangle$ and $|g\rangle$ are the atomic excited and ground states, respectively, and $|\psi_e\rangle$ and $|\psi_g\rangle$ are the corresponding field states. Defining a new coupling constant between the atom and the field as $\Gamma = g^2/2$ (with the dimensions of frequency), the equations of motion for these field states are

$$\frac{d}{dt}|\psi_e\rangle = -\sqrt{2\Gamma}A(t)|\psi_g\rangle \tag{3}$$

$$\frac{d}{dt}|\psi_g\rangle = \sqrt{2\Gamma}A^\dagger(t)|\psi_e\rangle. \tag{4}$$

In what follows we will assume that the atom is initially in the ground state. By integrating Eq. (4) and substituting in (3) one arrives at

$$\frac{d}{dt}|\psi_e\rangle = -\Gamma|\psi_e\rangle - 2\Gamma\int_{-\infty}^{t} dt' A^\dagger(t')A(t)|\psi_e\rangle - \sqrt{2\Gamma}A(t)|\psi_g(0)\rangle \tag{5}$$

after the commutator $[A(t), A^\dagger(t')] = \delta(t-t')$ is used to put the equation in normal order (note that only half of the δ function contributes, since the upper limit of integration is the point $t' = t$ itself). Again, Eq. (5) can be formally integrated (using $e^{\Gamma t}$ as an integrating factor) and substituted into itself to yield

$$|\psi_e\rangle = -\sqrt{2\Gamma}\int_{-\infty}^{t} dt' e^{-\Gamma(t-t')}A(t')|\psi_g(0)\rangle - 2\Gamma\int_{-\infty}^{t} dt' \times \int_{-\infty}^{t'} dt e^{-\Gamma(t-t')}A^\dagger(t)A(t')|\psi_e(t)\rangle. \tag{6}$$

This may be regarded as the beginning of a recursive solution that will eventually truncate if the initial state $|\psi_g(0)\rangle$ has a finite number of photons. The way to ensure this is, at every step of the iteration, to use the commutator $[A(t), A^\dagger(t')] = \delta(t-t')$ to put the expression in normal order. An essential point is that the δ functions turn out to be nested deep enough in the integral to give a vanishing contribution; that is, they produce terms that are only nonzero at one point, and thus have an integral of zero. As a result of this, there is only one new term at each step of the iteration, which, at the kth step, has k lowering operators acting directly on the initial state. Once $k = N$, the total number of excitations in the system, any successive terms will vanish. The first few terms of the series are given below.

$$|\psi_e\rangle = -\sqrt{2\Gamma}\int_{-\infty}^{t} dt_1 e^{-\Gamma(t-t_1)}A(t_1)|\psi_g(0)\rangle + (2\Gamma)^{3/2}\int_{-\infty}^{t} dt_1\int_{-\infty}^{t_1} dt_2\int_{-\infty}^{t_2} dt_3 e^{-\Gamma(t-t_1)}e^{-\Gamma(t_2-t_3)}A^\dagger(t_2)A(t_1)A(t_3)|\psi_g(0)\rangle - (2\Gamma)^{5/2}\int_{-\infty}^{t} dt_1\int_{-\infty}^{t_1} dt_2\int_{-\infty}^{t_2} dt_3\int_{-\infty}^{t_3} dt_4\int_{-\infty}^{t_4} dt_5 e^{-\Gamma(t-t_1)}e^{-\Gamma(t_2-t_3)}e^{-\Gamma(t_4-t_5)}A^\dagger(t_2)A^\dagger(t_4)A(t_1)A(t_3)A(t_5)|\psi_g(0)\rangle + \ldots. \tag{7}$$

The coefficient on the kth term is given by $(2\Gamma)^{k+\frac{1}{2}}(-1)^{k+1}$. Each successive term will have an integral with an extra $A^\dagger(t_k)e^{-\Gamma(t_k-t_{k+1})}A(t_{k+1})$. This can in principle be used to generate terms for any arbitrary $|\psi_g(0)\rangle$.

By substituting Eq. (7) into (4) and integrating one can express the final state of the field after all interaction with the atom has ceased (and the atom is, therefore, back to the ground state) as

$$\begin{aligned}|\psi_g(\infty)\rangle =& |\psi_g(0)\rangle - 2\Gamma\int_{-\infty}^{\infty} dt\int_{-\infty}^{t} dt_1 e^{-\Gamma(t-t_1)}A^\dagger(t)A(t_1)|\psi_g(0)\rangle \\ &+ (2\Gamma)^2\int_{-\infty}^{\infty} dt\int_{-\infty}^{t} dt_1\int_{-\infty}^{t_1} dt_2\int_{-\infty}^{t_2} dt_3 e^{-\Gamma(t-t_1)}e^{-\Gamma(t_2-t_3)}A^\dagger(t)A^\dagger(t_2)A(t_1)A(t_3)|\psi_g(0)\rangle \\ &- (2\Gamma)^3\int_{-\infty}^{\infty} dt\int_{-\infty}^{t} dt_1\int_{-\infty}^{t_1} dt_2\int_{-\infty}^{t_2} dt_3\int_{-\infty}^{t_3} dt_4\int_{-\infty}^{t_4} dt_5 e^{-\Gamma(t-t_1)}e^{-\Gamma(t_2-t_3)}e^{-\Gamma(t_4-t_5)} \\ &\times A^\dagger(t)A^\dagger(t_2)A^\dagger(t_4)A(t_1)A(t_3)A(t_5)|\psi_g(0)\rangle + \ldots.\end{aligned} \tag{8}$$

This equation may be used to get, in a very straightforward way, a full description of the state of the scattered field, as shown in Sec. II B.

B. Space-time description of a traveling two-photon field

For most of this paper we will restrict ourselves to two-photon fields, but essentially everything we present here can

be generalized to pulses with larger photon numbers in a straightforward way. We also start by considering traveling-wave fields, but the following section will show how standing wave fields can be dealt with as well.

For a traveling-wave multimode field in one dimension, the positive-frequency part of the electric field operator can be written as

$$E^{(+)}(\tau) = \mathcal{E} e^{-i\omega_0\tau} \int e^{-i\omega\tau} a_\omega = \mathcal{E} e^{-i\omega_0\tau} \sqrt{2\pi}\, A(\tau), \quad (9)$$

where $\tau = t \pm x/c$, depending on the wave's direction of travel, and $\mathcal{E} = \sqrt{\hbar\omega_0/2\epsilon_0}$; here ω_0 is the field's central frequency (we assume the field to be narrow band enough to ignore the dependence of $\mathcal{E}$ on ω), and, as above, ω represents a deviation from this central frequency. It is well known [15] that, for such a field, the probability $P(\tau_1,\tau_2)$ to detect two photons at the space-time points τ_1 and τ_2 is proportional to

$$P(\tau_1,\tau_2) \propto \|E^{(+)}(\tau_1)E^{(+)}(\tau_2)|\psi\rangle\|^2 \propto \|A(\tau_1)A(\tau_2)|\psi\rangle\|^2. \quad (10)$$

The most general two-photon state is given by

$$|\psi\rangle = \frac{1}{\sqrt{2}} \iint d\omega_1 d\omega_2 \tilde{f}(\omega_1,\omega_2) a^\dagger_{\omega_1} a^\dagger_{\omega_2} |0\rangle, \quad (11)$$

where without loss of generality we can assume the function $\tilde{f}(\omega_1,\omega_2)$ to be symmetric in ω_1,ω_2. We also assume the integral of $|\tilde{f}|^2$ is equal to 1. The action of $A(\tau_1)A(\tau_2)$ on this state is easily seen to be

$$A(\tau_1)A(\tau_2)|\psi\rangle = \sqrt{2} f(\tau_1,\tau_2)|0\rangle, \quad (12)$$

where

$$f(t_1,t_2) = \frac{1}{2\pi} \iint e^{-i(\omega_1 t_1 + \omega_2 t_2)} \tilde{f}(\omega_1,\omega_2)\, d\omega_1 d\omega_2 \quad (13)$$

is the two-dimensional Fourier transform of $f(\omega_1,\omega_2)$ (and may also be assumed to be symmetric in t_1, t_2). This makes the probability $P(\tau_a,\tau_b)$ of Eq. (10) directly proportional to $|f(\tau_a,\tau_b)|^2$, which means that $f(\tau_a,\tau_b)$ may be taken to be an effective two-photon wave function. The fact that photons do not strictly have wave functions in the Schrödinger sense means, primarily, that Eq. (10) is not an exact, fundamental result, but rather an approximation valid under certain conditions for certain kinds of photodetectors [16]; nonetheless, it is clear that the function $f(t_1,t_2)$ does contain all the information on the field state, regardless of whether its square can serve as a probability distribution or not.

In terms of $f(t_1,t_2)$, the state (11) can be written as

$$|\psi\rangle = \frac{1}{\sqrt{2}} \iint dt_1 dt_2 f(t_1,t_2) A^\dagger(t_1) A^\dagger(t_2)|0\rangle. \quad (14)$$

For the scattering problem that we introduced in the previous subsection, where the atom was implicitly assumed to be located at $z = 0$, the function $f_0(t_1,t_2)$ may be taken to describe the incoming field evolution at the atom's position, as a function of time. The outgoing field space-time wave function can then be obtained directly from Eq. (8) as follows. Direct substitution, and use of $[A(t),A^\dagger(t')] = \delta(t-t')$, yields

$$|\psi_g(\infty)\rangle = \frac{1}{\sqrt{2}} \int_{-\infty}^{\infty} dt_1 \int_{-\infty}^{\infty} dt_2 f_0(t_1,t_2) A^\dagger(t_1)A^\dagger(t_2)|0\rangle - 2\sqrt{2}\,\Gamma \int_{-\infty}^{\infty} dt \int_{-\infty}^{\infty} dt' \int_{-\infty}^{t} dt_1 e^{-\Gamma(t-t_1)} f_0(t_1,t') A^\dagger(t)A^\dagger(t')|0\rangle$$
$$+ 4\sqrt{2}\,\Gamma^2 \int_{-\infty}^{\infty} dt \int_{-\infty}^{t} dt_1 \int_{-\infty}^{t_1} dt_2 \int_{-\infty}^{t_2} dt_3 e^{-\Gamma(t-t_1)} e^{-\Gamma(t_2-t_3)} f_0(t_1,t_3) A^\dagger(t)A^\dagger(t_2)|0\rangle. \quad (15)$$

In this expression, the first two terms already have the desired form (the integral over t_1 in the second term provides the desired function of t,t'). The third term can be handled by introducing the Θ function $\Theta(t_1 - t_2)$ to extend the t_2 integral to $+\infty$, as a result of which the lower limit of the t_1 integral becomes equal to t_2 [with the understanding that t_2 must be less than t, which can be enforced explicitly by introducing another Θ function, $\Theta(t - t_2)$]. With this, and a suitable relabeling of the integration variables, the final result is seen to be of the form (14), with

$$f(t_1,t_2) = f_0(t_1,t_2) + f_1(t_1,t_2) + f_2(t_1,t_2)$$
$$f_1(t_1,t_2) = -4\Gamma \int_{-\infty}^{t_1} e^{-\Gamma(t_1-t')} f_0(t_2,t')\, dt'$$
$$f_2(t_1,t_2) = -2\Gamma\Theta(t_1-t_2) \int_{t_2}^{t_1} e^{-\Gamma(t_1-t')} f_1(t_2,t')\, dt'$$
$$= 8\Gamma^2\Theta(t_1-t_2) \int_{t_2}^{t_1} dt' e^{-\Gamma(t_1-t')} \times \int_{-\infty}^{t_2} dt'' e^{-\Gamma(t_2-t')} f_0(t'',t'). \quad (16)$$

In obtaining this result, use has been made of the symmetry assumed for f_0; although the solutions (16) for f_1 and f_2 do not themselves exhibit such a symmetry, one could certainly replace the expressions given by appropriately symmetrized ones.

The result (16) for f_1 is easy to interpret. It corresponds to a process in which one of the photons (the one indexed by the second argument, t_2) does not interact with the atom, whereas the other one, detected at t_1, was absorbed by the atom at an earlier time t' (and is reemitted at the time t_1 through an exponential decay rate Γ). The f_2 term, on the other hand, involves two such processes, but its form is a bit less transparent, so we will look at it in detail only for the simpler case in which the initial state of the field is unentangled (i.e., a product state).

Let, then, the initial state of the field be of the form (14) with $f_0(t_1,t_2) = f_0(t_1)f_0(t_2)$ (two uncorrelated but identical initial wave packets). Defining the function

$$G(t) = e^{-\Gamma t} \int_{-\infty}^{t} e^{\Gamma t'} f_0(t')dt' \quad (17)$$

[which is directly proportional to the single-photon excitation probability amplitude, as given by the first term in (7)], the result (16) reduces to

$$f(t_1,t_2) = f_0(t_1)f_0(t_2) - 4\Gamma f_0(t_2)G(t_1) + 8\Gamma^2\Theta(t_1-t_2) \times [G(t_1)G(t_2) - e^{-\Gamma(t_1-t_2)}G^2(t_2)] \quad (18)$$

[the last two terms come from splitting the integral from t_2 to t_1 in (16) into $\int_{-\infty}^{t_1} - \int_{-\infty}^{t_2}$]; or equivalently, in explicitly symmetric form,

$$f(t_1,t_2) = [f_0(t_1) - 2\Gamma G(t_1)][f_0(t_2) - 2\Gamma G(t_2)] - 4\Gamma^2 e^{-\Gamma|t_1-t_2|}G^2(t_<), \quad (19)$$

where $t_<$ is the smallest of t_1,t_2.

While the first term in Eq. (19) shows an explicitly factorizable state, the second one corresponds to a time-entangled (or frequency-entangled) state, which has been called a bound (as opposed to scattering) state by Shen and Fan [1] (it already appears in the work of Kojima *et al.* [9], where it is referred to as a nonlinear term). The idea is that, although the photons in such a state are (obviously) traveling away from the atom, they are still bound to each other in some sense. To be precise, the main characteristic of the bound state, as shown by Eq, (19), is that the probability to detect the photons separated by a time τ decreases exponentially with τ. In the one-directional geometry first considered by Shen and Fan (and which we are implicitly assuming in this section as well), this would naturally result in an exponential decrease of the two-photon wave function with the separation distance, which is what one expects from a bound state of two material particles.

We note that there has been a fair amount of research on two-photon bound states in other systems [17–19], and also a recent experimental demonstration [20]. We do not quite think the bound state in Eq. (19) belongs in this company; in fact, as we shall see in the next section, in the bidirectional case the two photons in this "bound" state could be detected arbitrarily far apart. In what follows, we shall refer to it as the entangled component of the scattering state,

$$f_{\rm ent}(t_1,t_2) \equiv -4\Gamma^2\, e^{-\Gamma|t_1-t_2|}G^2(t_<). \quad (20)$$

The strong correlation between the photons in this entangled component has been explained in Ref. [2] as resulting from the fact that they arrive at the atom sufficiently close in time for the first one to be absorbed and the second one to stimulate its reemission. The explicit form (20) suggests some nuances that are not perhaps entirely captured by this explanation. Note that the excitation probability amplitude $G(t)$ is evaluated twice with the same time argument, which suggests that the two photons are exciting the atom essentially simultaneously, at the earlier of the two times t_1 and t_2 (so one might as well speak of stimulated absorption as of stimulated emission here), and the only reason they may be detected at different times appears to be the finite lifetime, $1/\Gamma$, of the excited state.

We note also that a two-photon state described by a wave function of the form (20) can be seen as an instance of the time-entangled states considered by Franson [21], themselves very similar to the original Einstein-Podolsky-Rosen states [22]; the two properties that become simultaneously well defined in this state, as $\Gamma \to \infty$, are the total energy, proportional to $\omega_1 + \omega_2$ [see the expression (A5) in Appendix A], and the difference of the emission times $t_1 - t_2$. In the following sections we will show a number of schemes that may allow one to isolate this particular component of the state, at least in a conditional sense.

C. Higher photon numbers and extensions

Clearly, our fundamental result (8) can be used, along the same lines we have just shown, to deal with fields containing more than two photons, and derive explicit forms for the corresponding N-photon wave functions after interaction with the atom. In fact, with some care, one may even derive expressions for these quantities *during* the interaction, by making the upper limit of the outermost integrals in (8) equal to an arbitrary time rather than $+\infty$ [note, however, that while the interaction is happening the full state of the field also has a component associated with the atom being in the excited state, given by Eq. (7)] [23].

We shall not pursue these extensions in this paper, but we wish to mention here a possible simplification and an additional example. For an initial factorizable state that consists of N photons with identical wave packets, one may define

$$|N\rangle = \frac{1}{\sqrt{N!}}\left(\int \tilde{f}_0(\omega)a_\omega^\dagger\, d\omega\right)^N |0\rangle, \quad (21)$$

in which case it is easy to see that $A(t)|N\rangle = \sqrt{N}\, f_0(t)|N-1\rangle$. With this, repeated integration by parts allows one to cast the result (8) in the more compact form

$$\begin{aligned}|\psi_g(\infty)\rangle = {}& |N\rangle - 2\Gamma\sqrt{N}\int_{-\infty}^{\infty} dt_1\, G(t_1)A^\dagger(t_1)|N-1\rangle + (2\Gamma)^2\sqrt{N(N-1)}\int_{-\infty}^{\infty} dt_1\int_{-\infty}^{t_1} dt_2(G(t_1) \\ & - e^{-\Gamma(t_1-t_2)}G(t_2))G(t_2)A^\dagger(t_1)A^\dagger(t_2)|N-2\rangle - (2\Gamma)^3\sqrt{N(N-1)(N-2)}\int_{-\infty}^{\infty} dt_1\int_{-\infty}^{t_1} dt_2\int_{-\infty}^{t_2} dt_3(G(t_1) \\ & - e^{-\Gamma(t_1-t_2)}G(t_2))\big(G(t_2) - e^{-\Gamma(t_2-t_3)}G(t_3)\big)G(t_3)A^\dagger(t_1)A^\dagger(t_2)A^\dagger(t_3)|N-3\rangle + \ldots. \end{aligned} \quad (22)$$

From this, one can read directly the final N-photon wave function for any initial state $|N\rangle$, in nonsymmetric form (i.e., involving Θ functions). As an explicit example, the (partially symmetrized) result for $N = 3$ can be written as

$$\begin{aligned} f(t_1,t_2,t_3) = {}& \prod_{i=1}^{3}[f_0(t_i) - 2\Gamma G(t_i)] - (2\Gamma)^2\sum_{i=1}^{3} f(t_i)e^{-\Gamma|t_j-t_k|}G^2[\min(t_j,t_k)] \\ & + (2\Gamma)^3\sqrt{6}[e^{-\Gamma(t_2-t_3)}G(t_1)G^2(t_3) - e^{-\Gamma(t_1-t_3)}G(t_2)G^2(t_3) + e^{-\Gamma(t_1-t_2)}G^2(t_2)G(t_3)]\Theta(t_1-t_2)\Theta(t_2-t_3). \end{aligned} \quad (23)$$

Here, the first two terms are straightforward generalizations of the $N = 2$ case: the first one represents three independent one-photon processes where each photon has a probability amplitude of exciting or not exciting the atom (proportional to G and f_0, respectively), whereas the second term gives the two-photon excitation processes leading to entangled states like (20), only in the presence of a spectator photon. The last term, which has not been symmetrized, involves nonseparable (because of the Θ functions) three-photon excitations.

III. BIDIRECTIONAL WAVEGUIDE WITH A TWO-PHOTON INPUT

A. General formalism

In this section, we return to the two-photon case but consider a bidirectional waveguide, for which we introduce operators $A(t)$ and $B(t)$ to represent the sets of modes traveling in opposite directions. We take the underlying a_ω and b_ω operators to correspond to a spatial dependence $e^{i\omega x/c}$ (modes traveling to the right), and $e^{-i\omega x/c}$ (modes traveling to the left), respectively. At the atom's location, say $x = 0$, these modes overlap with a definite relative phase. The Hamiltonian will be

$$H = -i\hbar g\sigma_+[A(t) + B(t)] + i\hbar g\sigma_-[A^\dagger(t) + B^\dagger(t)]. \quad (24)$$

This can be put in the same form as the unidirectional case (1) by introducing the standing wave operators $c_\omega = (a_\omega + b_\omega)/\sqrt{2}$ and $d_\omega = (a_\omega - b_\omega)/\sqrt{2}$, since it is clear from (24) that the atom will only interact with the c-type operators. In terms of their multimode counterparts $C(t) = \frac{1}{\sqrt{2}}[A(t) + B(t)]$ and $D(t) = \frac{1}{\sqrt{2}}[A(t) - B(t)]$, we have

$$H = -i\hbar g\sqrt{2}(\sigma_+ C(t) - \sigma_- C^\dagger(t)). \quad (25)$$

This has the same form as (1) except for a $\sqrt{2}$ factor, so if we just define $\Gamma = g^2$ here, the same general solution (8) for the final field state will apply, only with A replaced by C throughout.

We will explicitly consider only initial unentangled states with M right-traveling and N left-traveling photons, in identically shaped wave packets, as follows:

$$|\psi_g(0)\rangle = |M,N\rangle \equiv \frac{1}{\sqrt{M!N!}}\left(\int \tilde{f}_0(\omega)a_\omega^\dagger\, d\omega\right)^M \times \left(\int \tilde{f}_0(\omega)b_\omega^\dagger\, d\omega\right)^N |0,0\rangle. \quad (26)$$

As in Sec. II B above, the function $\tilde{f}_0(\omega)$ gives the pulse's spectrum, and its Fourier transform, $f_0(t) = \frac{1}{\sqrt{2\pi}}\int \tilde{f}(\omega)e^{-i\omega t}\, d\omega$, the pulse's shape in the time domain. It is easy to verify that the action of $C(t)$ on the state (26) is

$$C(t)|M,N\rangle = \frac{f_0(t)}{\sqrt{2}}\left(\sqrt{M}|M-1,N\rangle + \sqrt{N}|M,N-1\rangle\right). \quad (27)$$

This can be used to work with the solution (8), as shown below.

B. Two photons arriving from the same direction ($M = 2, N = 0$)

Consider first an initial state of two identical right-traveling photons, $|\psi_g(0)\rangle = |2,0\rangle$. Substituting this into the equivalent of Eq. (8), with the operators $A, A^\dagger$ replaced by $C, C^\dagger$, and using the result (27), we obtain

$$|\psi_g(\infty)\rangle = |2,0\rangle - 2\Gamma\int_{-\infty}^{\infty} dt G(t)C^\dagger(t)|1,0\rangle + 2\sqrt{2}\Gamma^2 \times \int_{-\infty}^{\infty} dt \int_{-\infty}^{t} dt' G(t')[G(t) - e^{\Gamma(t'-t)}G(t')]C^\dagger(t)C^\dagger(t')|0,0\rangle \quad (28)$$

in terms of the function G of Eq. (17).

We may now rewrite the $C^\dagger$ operators, and also the states $|2,0\rangle$ and $|1,0\rangle$, in terms of $A^\dagger$ and $B^\dagger$, with the result

$$|\psi_g(\infty)\rangle = \int dt_1 \int dt_2 \left(\frac{1}{\sqrt{2}} f_{a_{2,0}}(t_1,t_2)A^\dagger(t_1)A^\dagger(t_2) + \frac{1}{\sqrt{2}} f_{b_{2,0}}(t_1,t_2)B^\dagger(t_1)B^\dagger(t_2) + f_{\mathrm{split}_{2,0}}(t_1,t_2)A^\dagger(t_1)B^\dagger(t_2)\right)|0\rangle, \quad (29)$$

which shows a part involving two transmitted (a) photons, a part involving two reflected (b) photons, and a split part, containing one of each. The factors of $1/\sqrt{2}$ arise from the normalization introduced in Eq. (26) above. The corresponding amplitudes are

$$\begin{aligned} f_{a_{2,0}}(t_1,t_2) &= [f_0(t_1) - \Gamma G(t_1)][f_0(t_2) - \Gamma G(t_2)] + \frac{1}{4} f_{\mathrm{ent}}(t_1,t_2) \\ f_{b_{2,0}}(t_1,t_2) &= \Gamma^2 G(t_1)G(t_2) + \frac{1}{4} f_{\mathrm{ent}}(t_1,t_2) \\ f_{\mathrm{split}_{2,0}}(t_1,t_2) &= -\sqrt{2}\,\Gamma[f_0(t_1) - \Gamma G(t_1)]G(t_2) + \frac{\sqrt{2}}{4} f_{\mathrm{ent}}(t_1,t_2). \end{aligned} \quad (30)$$

Here, f_a and f_b are given in explicitly symmetric form, but f_{split} is asymmetric: the reflected photon (indexed by t_2) has a different pulse profile than the transmitted one.

Recalling that $G(t)$ gives the single-photon probability amplitude to excite the atom, the results (30) make sense intuitively. For instance, the only way to get a reflected (b) photon is to excite the atom (and then have the photon be emitted into the left-traveling mode), whereas a transmitted (a) photon may (the G term) or may not (the f_0 term) result from an excitation event. Note that the entangled component contributes to all the possible outcomes, and so, in particular, for the split case one may find the two photons described by this term very far apart, provided only $|\tau_1 - \tau_2| = |t_1 - t_2 - x_1 - x_2|$ is sufficiently small.

For an initial Gaussian wave packet defined by

$$f_0(t) = \frac{1}{\sqrt{T\sqrt{2\pi}}} e^{-t^2/4T^2} \quad (31)$$

the function $G(t)$ is given by [24]

$$G(t) = \sqrt[4]{\frac{\pi}{2}}\sqrt{T}\, e^{\Gamma^2T^2} e^{-\Gamma t}\left[\mathrm{erf}\left(\frac{t}{2T} - \Gamma T\right) + 1\right]. \quad (32)$$

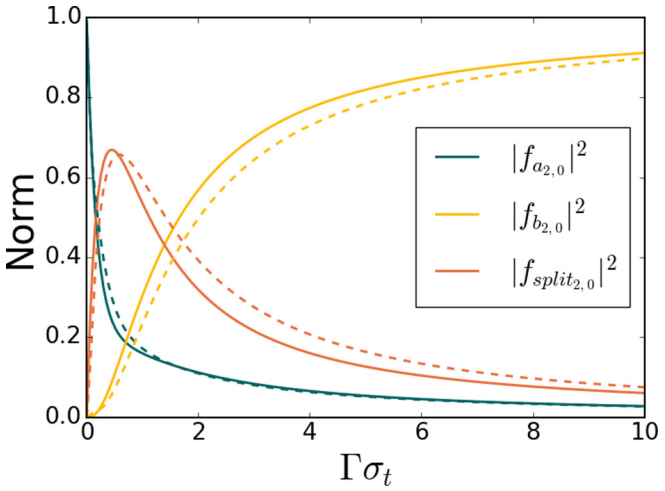

FIG. 1. The probabilities to find the two photons in the right-traveling modes, left-traveling modes, or one left and one right mode, after interacting with the atom, as a function of $\Gamma\sigma_t$ for the Gaussian pulse (solid line) and the flat-top pulse (dashed line).

We have also carried out calculations with a smooth square (or flat-top) pulse defined by

$$f_0(t) = \frac{1}{2\sqrt{\mathcal{N}}}(\mathrm{erf}[a(t-t_0)] - \mathrm{erf}[a(t-\mathcal{T}-t_0)]), \quad (33)$$

where the normalization factor is

$$\mathcal{N} = \frac{1}{a}\sqrt{\frac{2}{\pi}}\left(e^{-a^2\mathcal{T}^2/2}-1\right) + \mathcal{T}\,\mathrm{erf}\left(\frac{a\mathcal{T}}{\sqrt{2}}\right). \quad (34)$$

Here, the parameter a (which we set equal to 1 in what follows) gives the rate at which the pulse rises, and $\mathcal{T}$ gives the pulse's approximate width. A more precise definition of the width, which allows for a fair comparison to the Gaussian pulse, is provided by the standard deviation $\sigma_t \equiv [\int dt f^2(t) t^2]^{1/2}$. As will be shown, using this gives comparable results for the two kinds of pulses as a function of the dimensionless coupling parameter $\Gamma\sigma_t$. For the Gaussian pulse, one just has $\sigma_t = T$, whereas for the flat-top pulse we find $\sigma_t \simeq 0.283\mathcal{T} - 0.098$ for $\mathcal{T}$ greater than about 5.

For the flat-top pulse the function $G(t)$ can also be calculated analytically:

$$G(t) = \frac{e^{-\Gamma t}}{2\Gamma\sqrt{\mathcal{N}}}\left[e^{\Gamma(4a(t_0+\mathcal{T})+\Gamma)/4a^2}\mathrm{erfc}\left(\frac{\Gamma}{2a} - a(t-t_0-\mathcal{T})\right)\right.$$
$$\left. - e^{\Gamma(4at_0+\Gamma)/4a^2}\mathrm{erfc}\left(\frac{\Gamma}{2a} - a(t-t_0)\right)\right] + \frac{f_0(t)}{\Gamma}. \quad (35)$$

For any pulse shape, the norm of each of the components in Eq. (30) ($f_{a_{2,0}}$, $f_{b_{2,0}}$, or $f_{\mathrm{split}_{2,0}}$) reflects the overall probability of the corresponding process. Figure 1 shows these probabilities for both kinds of pulses, plotted against the dimensionless coupling parameter $\Gamma\sigma_t$ [25].

As the figure shows, for sufficiently large coupling strength or pulse duration both photons will be reflected with a probability that approaches one. On the other hand, for a small-coupling regime or a medium pulse width we have that there is a maximum probability of .669 for the photons to be split equally among both directions of the waveguide. Finally, for very small coupling or for short pulses we see that the photons tend to be transmitted through the waveguide with probability that approaches one.

Besides looking at these overall transmission and reflection probabilities, we can use the amplitudes of the components in Eq. (30) to look at the photon detection probabilities at specific space-time points τ_1, τ_2, as explained at the beginning of Sec. II B. The squares of the two-time amplitudes give directly the two-photon detection probabilities, whereas the single-photon detection probabilities can be calculated as follows:

$$P_a(\tau) \propto \|E^{(+)}(\tau)|\psi\rangle\|^2 \propto \|A(\tau)|\psi\rangle\|^2$$
$$\propto \left\| \sqrt{2}\int_{-\infty}^{\infty} d\tau'\, f_a(\tau,\tau')A^\dagger(\tau')|0\rangle \right.$$
$$\left. + \int_{-\infty}^{\infty} d\tau'\, f_{\mathrm{split}}(\tau,\tau')B^\dagger(\tau')|0\rangle \right\|^2$$
$$\propto \int_{-\infty}^{\infty} d\tau' \left(2|f_a(\tau,\tau')|^2 + |f_{\mathrm{split}}(\tau,\tau')|^2\right) \quad (36)$$

(and similarly for the reflected modes). The results are shown in Figs. 2 and 3 below, for a Gaussian pulse.

As expected from the results in Fig. 1, in the weak-coupling regime the photons are primarily transmitted and in the strong-coupling regime they are nearly always reflected.

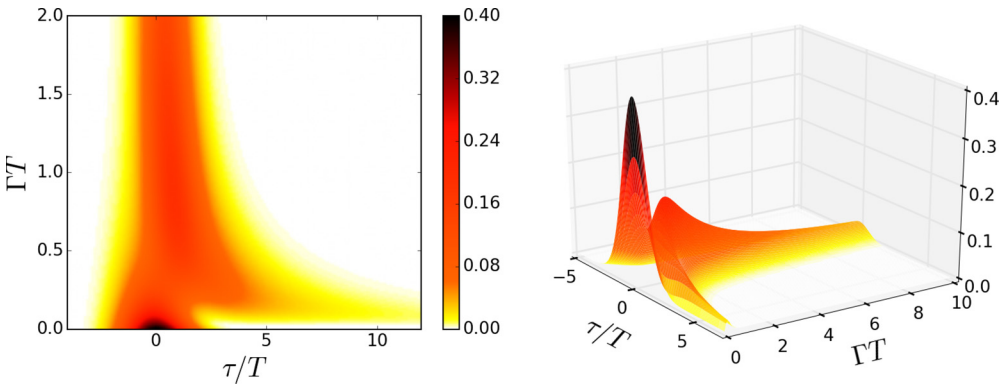

FIG. 2. Contour plot and 3D plot of $\langle A^\dagger A\rangle$ (in units of $1/T$) for an input Gaussian pulse as a function of Γ and space-time position along the pulse, τ. Note the expanded range of Γ in the plot on the right.

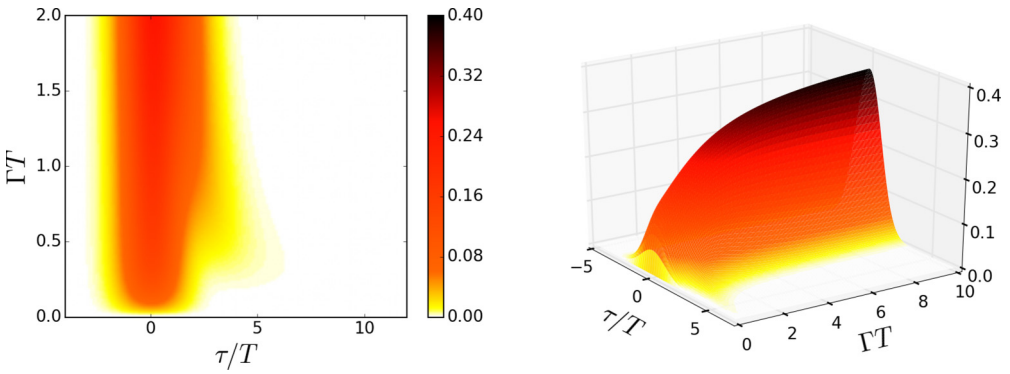

FIG. 3. Contour plot and 3D plot of $\langle B^\dagger B\rangle$ (in units of $1/T$) for an input Gaussian pulse as a function of Γ and space-time position along the pulse, τ. Note the expanded range of Γ in the plot on the right.

There is also some amount of pulse distortion, which is most pronounced for relatively small coupling, of the order of $\Gamma T \sim 0.1$–0.4 for the reflected pulse. In this region, the pulse widens, at some point even displaying a double maximum, and correspondingly the probability density as a function of τ goes down.

The results for a flat-top pulse are shown in Figs. 4 and 5 below.

The flat-top pulse behaves in much the same way as the Gaussian pulse, although the change in shape is perhaps more pronounced. For large values of $\Gamma\sigma_t$, both the reflected and transmitted pulses become again nearly square, but for smaller values the square shape is almost completely lost, especially for the transmitted pulse.

Further insight is obtained from a look at the two-photon detection probabilities, shown for the Gaussian pulse in Fig. 6. These are calculated as indicated at the beginning of Sec. II B [see in particular Eq. (10)], only separately for the three scenarios considered, that is, as proportional to $\|A(\tau_1)A(\tau_2)|\psi\rangle\|^2$, $\|A(\tau_1)B(\tau_2)|\psi\rangle\|^2$, and $\|B(\tau_1)B(\tau_2)|\psi\rangle\|^2$, respectively [26]. Note that the first and third of these are proportional to $2|f_a|^2$ and $2|f_b|^2$, whereas the second one is proportional to $|f_{\rm split}|^2$ only, without the factor of 2. This follows immediately from Eq. (12) and its equivalent with $A(\tau_1)A(\tau_2)$ replaced by $A(\tau_1)B(\tau_2)$. Hence, in order to properly compare the final probability distributions, we should either multiply $|f_a|^2$ and $|f_b|^2$ by 2 or divide $|f_{\rm split}|^2$ by 2, and we have adopted the latter approach for simplicity.

As can be seen, for small ΓT, when the pulse is primarily transmitted or split, the two-photon detection probabilities show a relatively large component that is delayed in time; for the split case, this is associated primarily with the reflected photon. The delay becomes less significant as the coupling increases, or alternatively as the pulse becomes longer (increasing ΓT). As this happens, the detection probability for two reflected (B) photons, consisting of two components symmetrically delayed relative to the original pulse, increases, while the other two distributions become narrower. For very large ΓT, the split and transmitted modes exhibit very sharply bunched peaks, whereas the probability of two reflected photons comes to resemble the original pulse, only with a thin slice cut out, which is indicative of antibunching, as $f_b(\tau,\tau) = 0$. This is effectively due to destructive interference between the entangled and unentangled components of f_b [compare Eqs. (30) and (20), with $t_1 = t_2$].

The corresponding probabilities for the flat-top pulse are plotted in Fig. 7.

Although this figure shows a pattern similar to the one exhibited in Fig. 6, the presence of relatively well-defined edges makes a clear difference. Features such as the ones exhibited in Fig. 6(d) tend now to spread along or concentrate at the (trailing) edges [as in Fig. 7(a) or Fig. 7(d)]. Figure 7(g) shows

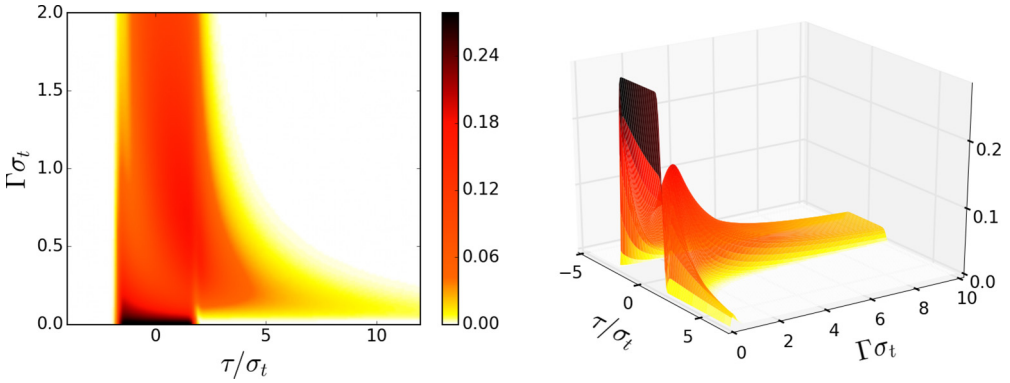

FIG. 4. Contour plot and 3D plot of $\langle A^\dagger A\rangle$ (in units of $1/\sigma_t$) for an input flat-top pulse as a function of Γ and space-time position along the pulse, τ. Note the expanded range of Γ in the plot on the right.

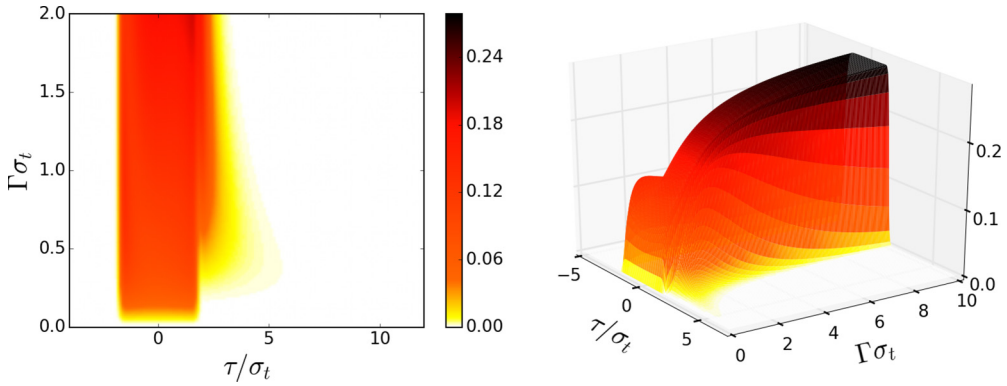

FIG. 5. Contour plot and 3D plot of $\langle B^\dagger B\rangle$ (in units of $1/\sigma_t$) for an input flat-top pulse as a function of Γ and space-time position along the pulse, τ. Note the expanded range of Γ in the plot on the right.

a definite tendency for the two reflected photons to be detected near one or the other edge of the pulse, whereas Figs. 7(h) and 7(k) show that although there is a large probability to find the two photons approximately together somewhere inside the pulse, there is also an appreciable probability to find the transmitted photon inside and the reflected one near the edge of the pulse. (Compare these results with the similar edge effects predicted for sharp square pulses in Ref. [9].)

C. Two photons arriving from opposite directions ($M = 1, N = 1$)

Instead of a two-photon pulse traveling from either the right or left, we may also consider the case in which one photon comes in from the right and another from the left, a situation that has recently been described by Roulet *et al.* as two photons incident on an atomic beam splitter [8] (see also Ref. [12]). This initial state can be expressed as

$$\begin{aligned}|1,1\rangle &= \int_{-\infty}^{\infty} dt_1 \int_{-\infty}^{\infty} dt_2\, f_0(t_1) f_0(t_2) A^\dagger(t_1) B^\dagger(t_2)|0,0\rangle \\ &= \frac{1}{2}\int_{-\infty}^{\infty} dt_1 \int_{-\infty}^{\infty} dt_2\, f_0(t_1) f_0(t_2)(C^\dagger(t_1)C^\dagger(t_2) \\ &\quad - D^\dagger(t_1)D^\dagger(t_2))|0,0\rangle. \end{aligned} \tag{37}$$

The lack of cross terms makes this state's evolution particularly simple: the final result will be equivalent to a unidirectional waveguide transformation for the C modes, plus the D component unchanged. When written back in terms of the A and B modes, the result is:

$$\begin{aligned} f_{a_{1,1}}(t_1,t_2) = f_{b_{1,1}}(t_1,t_2) &= \frac{1}{\sqrt{2}}\Big(-\Gamma G(t_1)[f_0(t_2)-\Gamma G(t_2)] \\ &\quad - [f_0(t_1)-\Gamma G(t_1)]\Gamma G(t_2) + \frac{1}{2} f_{\text{ent}}(t_1,t_2)\Big) \\ f_{\text{split}_{1,1}}(t_1,t_2) &= [f_0(t_1)-\Gamma G(t_1)][f_0(t_2)-\Gamma G(t_2)] \\ &\quad + \Gamma^2 G(t_1)G(t_2) + \frac{1}{2} f_{\text{ent}}(t_1,t_2). \end{aligned} \tag{38}$$

The second of these terms, $f_{\text{split}_{1,1}}$, has been studied in considerable detail in Ref. [8].

When the result (38) is compared to the $|2,0\rangle$ case [Eqs. (30)], one can see that the case where the two photons leave in the same direction in (38) is actually the sum of two symmetric split processes from (30), which makes sense, since those represented processes in which one photon was reflected and the other one transmitted. Similarly, the split case in (38) is actually the sum of the two reflected and two transmitted cases in (30), which also makes sense, since these are the processes that lead to a split scenario for the $|1,1\rangle$ state. These results are perhaps easiest to see from the frequency-domain formulas shown in Appendix A.

Note, however, that the addition of the various alternatives happens at the level of the probability *amplitudes*, and so the actual total probabilities of the various processes are not, in general, additive. This can be seen from Fig. 8 below, which shows the probabilities calculated from (38). The probability of a split scenario in Fig. 8 is not simply equal to the sum of the probabilities for two reflections and two transmissions in Fig. 1, although it is qualitatively similar (and vice versa).

Specifically, we see that for both strong and weak coupling (or long and short pulses) the most likely outcome is that one photon leaves the waveguide in each path. The probability for two photons to leave in the same direction peaks at $\Gamma T = .586$ (for the Gaussian pulse) with a value of .444 for each direction, or .888 total; correspondingly, the probability to find one photon in each arm reaches a minimum of .111 at the same point. It is somewhat interesting that, while the two-level atom may act like a perfect mirror for two photons approaching from the same direction (large-coupling limit in Fig. 1), it comes close to but never quite acts as a perfect 50-50 beam splitter when two photons approach from opposite directions, since such a beam splitter would always send both photons out along the same direction [27]. (We note, however, that very recently Roulet *et al.* have shown that this kind of behavior is, in fact, exhibited for this system for an appropriate detuning [8].) As before, the two kinds of pulses considered yield very similar results when $\Gamma\sigma_t$ is adopted as a measure of the coupling strength.

As in Sec. III B, we may expand this picture by looking at the space-time dependence of the photon detection probabilities. Clearly, for single-photon detection the result (36) will again apply, only with the appropriate functions f_a and f_{split}. In this case, because of the symmetry of the initial state, there is no difference between the single-photon detection probabilities in the right-traveling versus the left-traveling

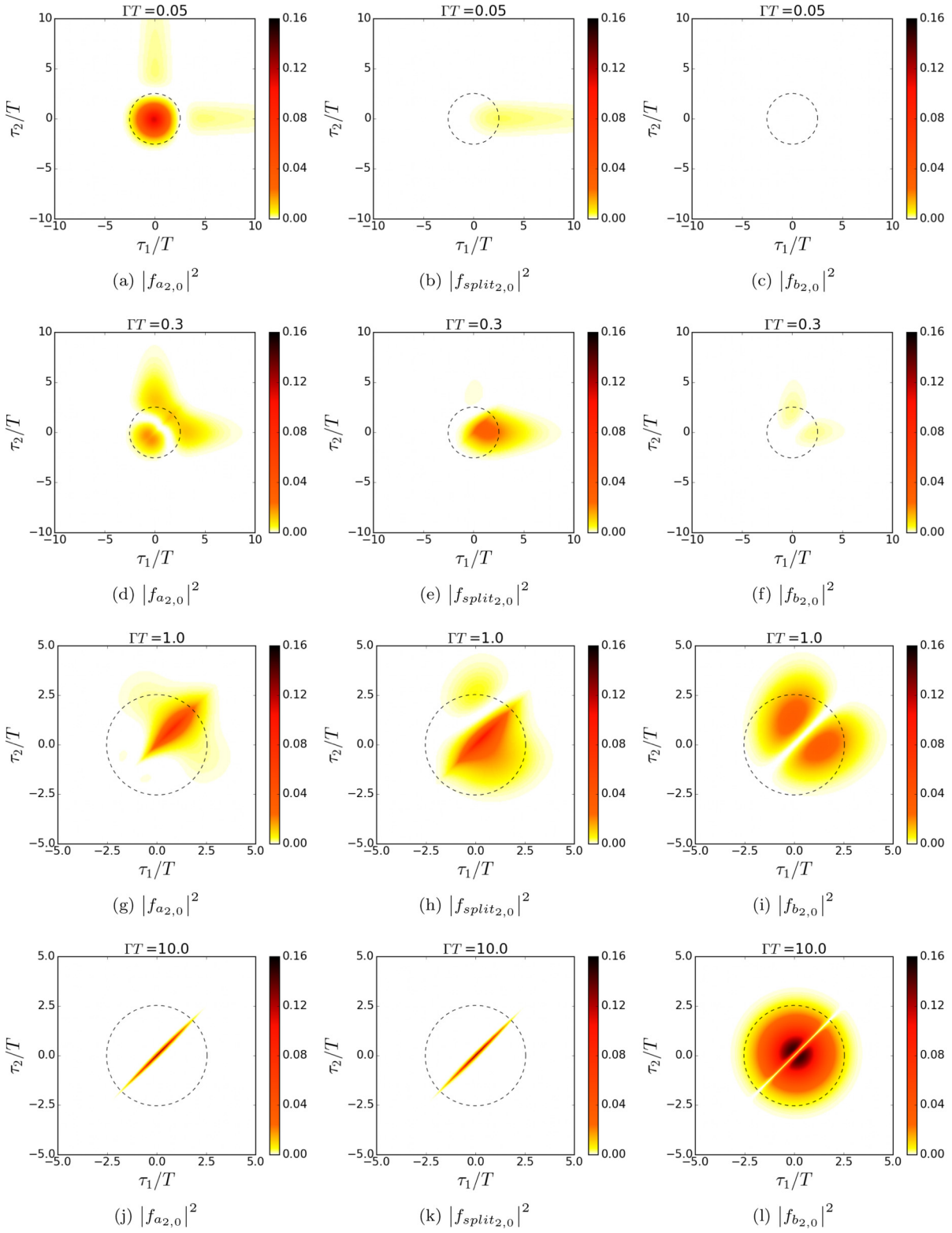

FIG. 6. Probabilities for detecting two photons in the A modes (both transmitted, leftmost column), B modes (both reflected, rightmost column), or one in each (middle column, where the index τ_1 labels the transmitted, and τ_2 the reflected, photon). Γ is as labeled. Note that the scale is not the same for each image, but the dotted circle indicates in each case the area of the initial pulse. The density scale is in units of $1/T^2$.

modes. These probabilities are plotted for the Gaussian in Fig. 9 and for the flat-top pulse in Fig. 10. Again there is a dip and a broadening of the pulse around the same values of $\Gamma\sigma_t$ as in the $M = 2, N = 0$ case.

The two-photon detection probabilities are plotted in Fig. 11 for the Gaussian pulse, and in Fig. 12 for the flat-top pulse.

Looking at the Gaussian case first, we see that the effect on the pulse for this case is very similar to that of the $M = 2, N =$

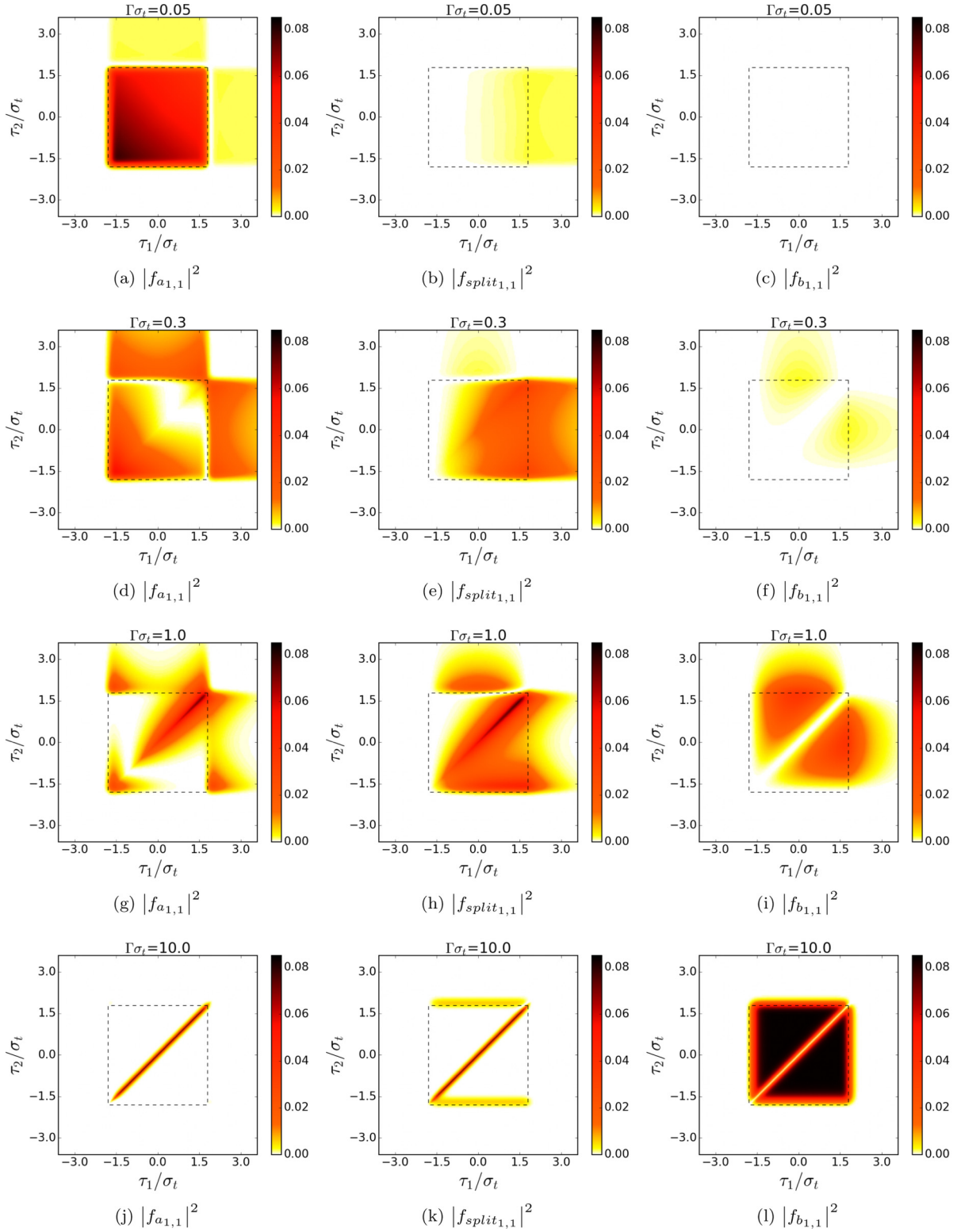

FIG. 7. The same as for Fig. 6, but for a smooth square pulse. Note that the dotted square corresponds to the area of the initial pulse in all images. The density scale is in units of $1/\sigma_t^2$.

0 case, with the primary difference being the approximate switching of probabilities between the split case and the sum of the other two. For small coupling, the split mode reproduces the incoming pulse. As Γ increases, the two-reflected and two-transmitted probabilities become, for a while, the dominant processes, while the split mode probability develops a shape similar to the transmitted pulse in Fig. 6(d). In the large ΓT limit, on the other hand, we again find two highly bunched probability distributions, this time for the two-reflected and two-transmitted cases, and an antibunched one for the split

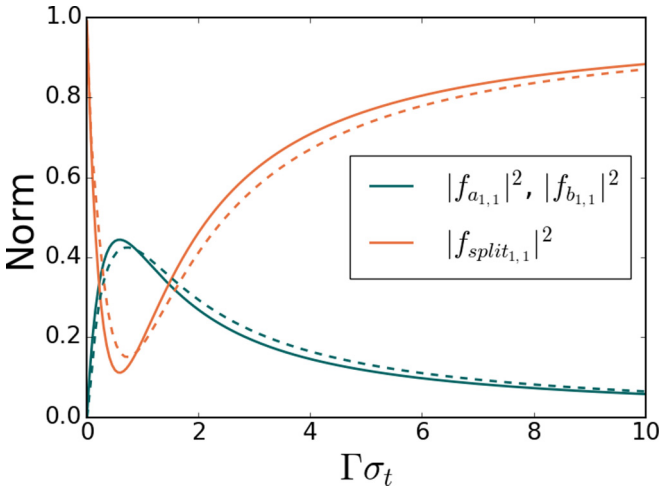

FIG. 8. The probabilities of the various outcomes upon interacting with the atom as a function of $\Gamma\sigma_t$ for the Gaussian pulse (solid line) and the flat top pulse (dashed line). Note that the probabilities for the two photons to end in the left and right modes are equal and thus on top of one another in this plot.

case, although unlike in the previous subsection the latter does not go all the way to zero at $\tau_1 = \tau_2$. (See the analytical results in Sec. III D.)

The flat-top pulse results again show pronounced edge effects, but now, because of the initial symmetry of the problem, there is no difference between the transmitted and the reflected photon.

As before, some of these results may be found in recent works as well. The reader is invited to compare the rightmost picture on the top row of Fig. 6 of Ref. [12] to a combination of our Figs. 11(g)–11(i), whereas the top row of Fig. 7 of Ref. [8] corresponds essentially to the middle column of our Fig. 12.

D. Adiabatic approximation

In order to better understand many of the results we have presented above, it is useful to consider the adiabatic limit, namely, the case of a long pulse. For the Gaussian pulse, the only timescale that T can be compared to is provided by $1/\Gamma$, so to express the requirement that T be large we must require $\Gamma T \gg 1$; accordingly, for this problem, the adiabatic limit can also be thought of as the strong-coupling limit.

In general, the function $G(t)$ can be expressed in terms of the derivatives of $f(t)$ by repeatedly integrating Eq. (17) by parts, with $dv = e^{\Gamma t'}dt'$ and $u = f^{(i)}(t)$. This yields the

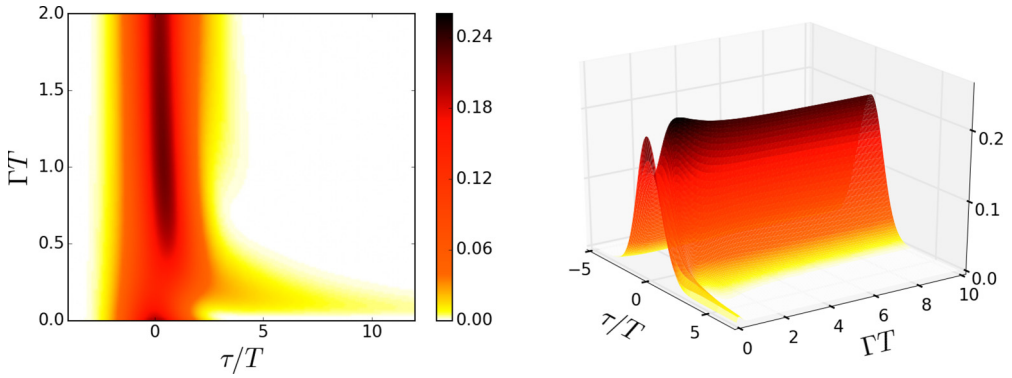

FIG. 9. Contour plot and 3D plot of $\langle A^\dagger A\rangle$ or $\langle B^\dagger B\rangle$ (in units of $1/T$) for an input Gaussian pulse as a function of Γ and space-time position along the pulse, τ. Note the expanded range of Γ in the plot on the right.

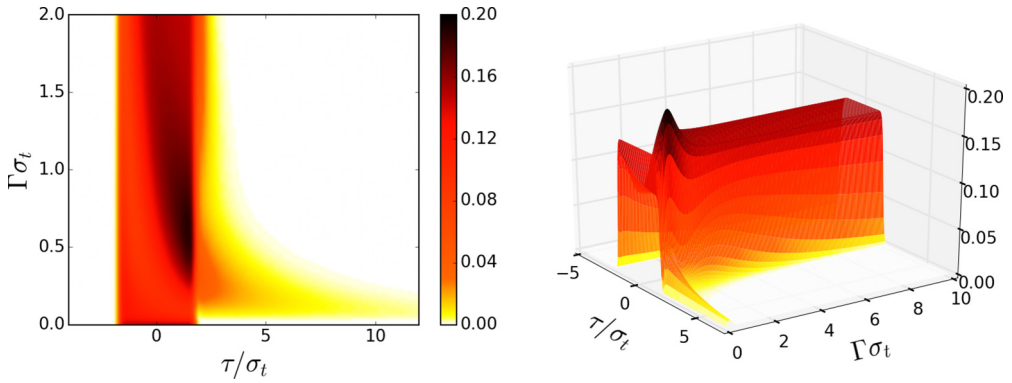

FIG. 10. Contour plot and 3D plot of $\langle A^\dagger A\rangle$ or $\langle B^\dagger B\rangle$ (in units of $1/\sigma_t$) for an input flat top pulse as a function of Γ and space-time position along the pulse, τ. Note the expanded range of Γ in the plot on the right.

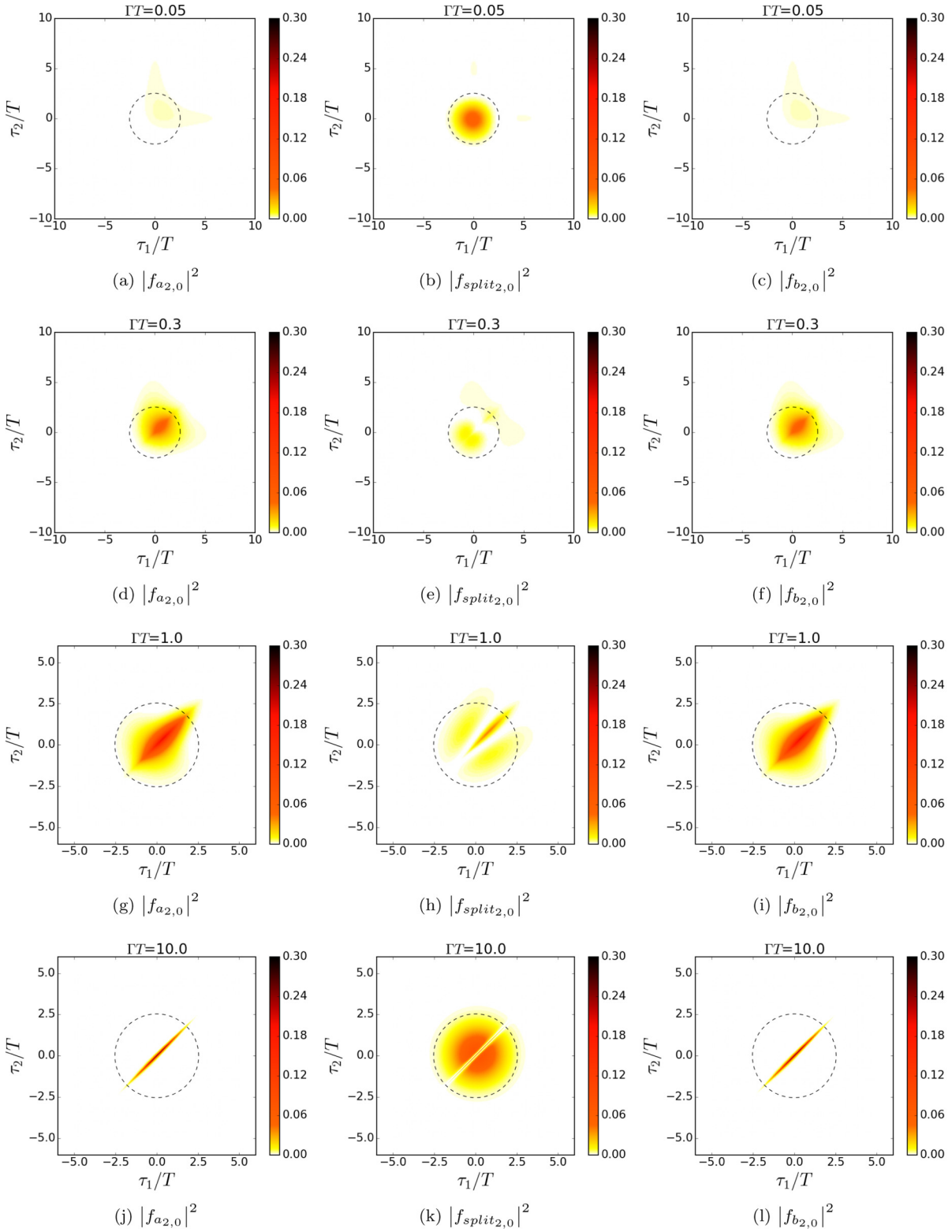

FIG. 11. Probabilities for detecting two photons in the A modes (both transmitted, leftmost column), B modes (both reflected, rightmost column), or one in each (middle column). Γ is as labeled. Note that the scale is not the same for each image, but the dotted circle indicates in each case the area of the initial pulse. The density scale is in units of $1/T^2$.

following series:

$$G(t) \approx \sum_{i=0}^{n} \frac{(-1)^i}{\Gamma^{i+1}} f^{(i)}(t). \tag{39}$$

For a simple pulse like the Gaussian we expect each derivative with respect to t to bring down a factor of $1/T$. Hence, in the adiabatic, or strong-coupling, regime, we may neglect the higher-order terms and keep only the first few, say up to $n = 1$.

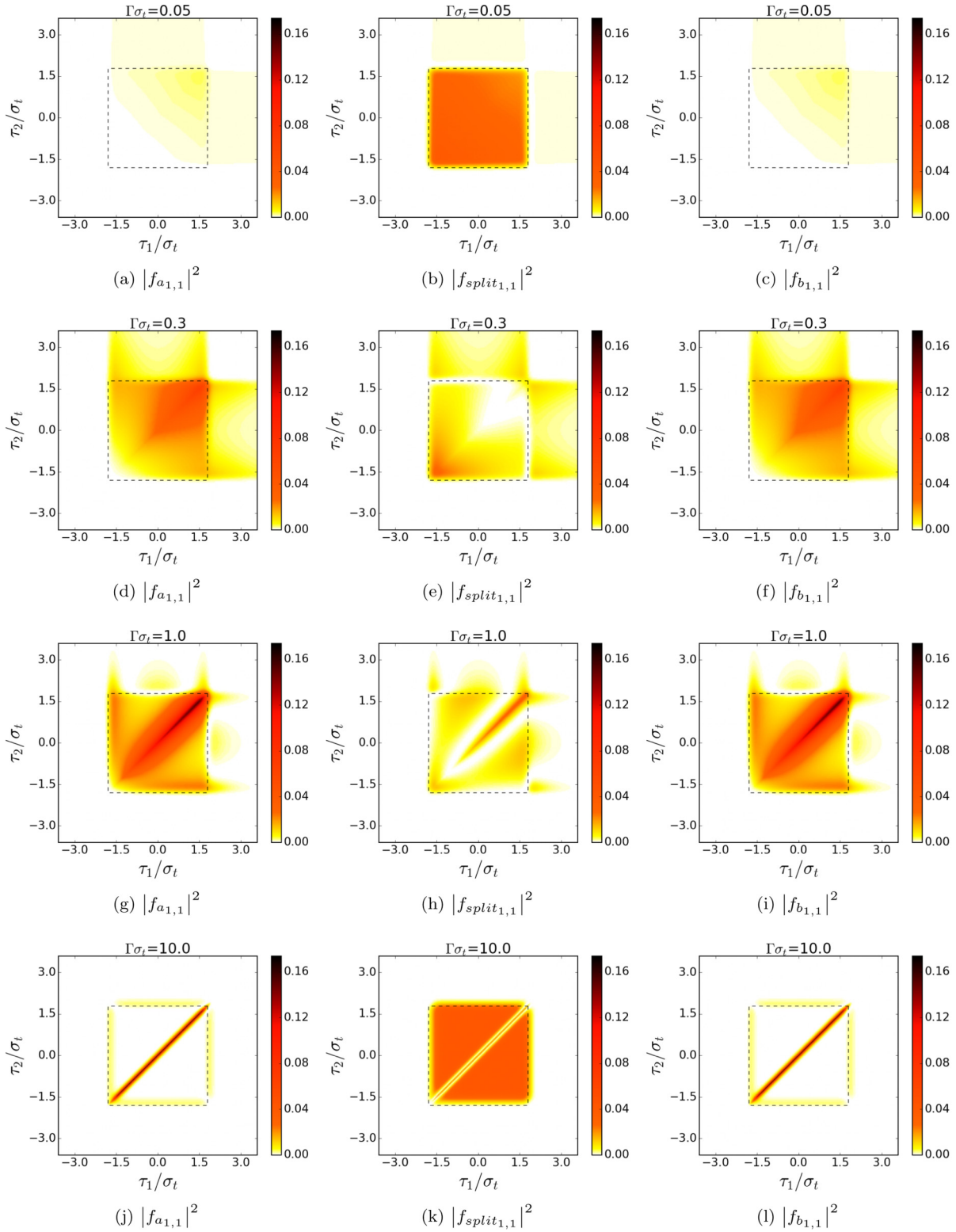

FIG. 12. The same as for Fig. 11, but for a smooth square pulse. Note that the dotted square corresponds to the area of the initial pulse in all images. The density scale is in units of σ_t^2.

In that case,

$$G(t) \approx \frac{f(t)}{\Gamma} - \frac{f'(t)}{\Gamma^2} \tag{40}$$

and the entangled term of Eq. (20) becomes

$$f_{\text{ent}}(t_1,t_2) \approx 4 f(t_<) e^{-\Gamma|t_1-t_2|}\left(\frac{2f'(t_<)}{\Gamma} - f(t_<)\right). \tag{41}$$

With this, for the $M = 2, N = 0$ case we can express Eqs. (30) as

$$f_{a_{2,0}}(t_1,t_2) \approx \frac{f_{\rm ent}(t_1,t_2)}{4} \tag{42}$$

$$f_{b_{2,0}}(t_1,t_2) \approx f(t_1)f(t_2) - \frac{f(t_1)f'(t_2)}{\Gamma} - \frac{f(t_2)f'(t_1)}{\Gamma} + \frac{f_{\rm ent}(t_1,t_2)}{4} \tag{43}$$

$$f_{{\rm split}_{2,0}}(t_1,t_2) \approx -\frac{\sqrt{2}}{\Gamma} f(t_1)f'(t_2) + \frac{\sqrt{2}}{4} f_{\rm ent}(t_1,t_2). \tag{44}$$

From Eqs. (42) and (44) is clear that as Γ becomes very large, the entangled component of the wave function is responsible for the strong bunching effects in the transmitted and split modes. In particular, Figs. 6(j), 6(k) and 7(j), 7(k) show, essentially, the two-photon detection probability associated with this entangled component. Observation of the entangled state is therefore possible, in principle, in this system, most easily by selecting for events where both photons are detected in the transmitted channel.

On the other hand, Eq. (43) shows how the reflected mode closely reproduces the initial pulse, as the first term is just the input spectrum and the derivative terms will be small if Γ is large. There is, however, a missing piece to the pulse, as is apparent from Figs. 6(l) and 7(l), again because of the entangled component (41); in fact, it is clear from these equations that, no matter how large Γ becomes, the pulse will always be maximally antibunched ($f_{b_{2,0}} = 0$), when $t_1 = t_2$, although the width of this slice does decrease with increasing Γ.

The results (42)–(44) also explain, at least mathematically, the edge effects observed in Fig. 7 for the flat-top pulse. Indeed, for this kind of pulse, $f'(t)$ is maximum around the pulse's edge [consider Eq. (33) with $a\mathcal{T} \gg 1$], and so a term such as $f(t_1)f'(t_2)/\Gamma$ in Eq. (44) yields precisely what Fig. 7(k) shows: the photon described by the argument t_1 (or τ_1 in the figure) is most likely to be located anywhere inside the pulse, but the one described by t_2 (τ_2) has a significant probability to be found at the pulse's edge.

Similarly, for the $M = 1, N = 1$ case we have the following approximations:

$$f_{a_{1,1}}(t_1,t_2) = f_{b_{1,1}}(t_1,t_2) \approx \frac{1}{\sqrt{2}}\left[- \frac{f(t_1)f'(t_2)}{\Gamma} - \frac{f(t_2)f'(t_1)}{\Gamma} + \frac{f_{\rm ent}(t_1,t_2)}{2}\right] \tag{45}$$

$$f_{{\rm split}_{1,1}}(t_1,t_2) \approx f(t_1)f(t_2) - \frac{f(t_1)f'(t_2)}{\Gamma} - \frac{f(t_2)f'(t_1)}{\Gamma} + \frac{f_{\rm ent}(t_1,t_2)}{2}. \tag{46}$$

Now the entangled component dominates, for large enough coupling, the reflected and transmitted modes, and it is the split modes that reproduce the initial spectrum with a dip at $t_1 = t_2$. Note, however, that, since there is a factor of $\frac{1}{2}$ rather than $\frac{1}{4}$ on the $f_{\rm ent}$ term, the function $f_{{\rm split}_{1,1}}(t_1,t_2)$ does not go all the way to zero at $t_1 = t_2$.

By using Eqs. (42)–(46) we can also approximate to order $1/\Gamma$ the single detection probability for $|\psi_0\rangle = |2,0\rangle$ as

$$\langle\psi|A^\dagger A|\psi\rangle \approx \frac{2}{\Gamma} f^4(\tau) \tag{47}$$

$$\langle\psi|B^\dagger B|\psi\rangle \approx f^2(\tau) + \frac{f^4(\tau)}{\Gamma} - \frac{2}{\Gamma} f(\tau)f'(\tau) \tag{48}$$

and similarly when $|\psi_0\rangle = |1,1\rangle$ the single detection probability becomes

$$\langle\psi|B^\dagger B|\psi\rangle = \langle\psi|A^\dagger A|\psi\rangle \approx \frac{f^2(\tau)}{2} + \frac{4}{\Gamma} f^4(\tau) - \frac{f(\tau)f'(\tau)}{\Gamma}. \tag{49}$$

IV. CONCLUSIONS

We have presented a formal solution for the evolution of a quantized field interacting with a two-level atom in a one-dimensional setting (waveguide) that is valid for an arbitrary number of photons and directly yields expressions for the outgoing N-photon wave functions, given an (also arbitrary) input pulse. We have illustrated our results for the case of a two-photon pulse, with examples for bidirectional and unidirectional waveguides, and calculated the one- and two-photon detection probabilities in the final state, explicitly, for two kinds of input pulses, Gaussian and flat-top. We have also derived simplified analytical results for the large-coupling limit.

We believe that this method can be used to obtain useful insights for a number of systems of interest in quantum optics and quantum information, and intend to apply it to such systems in the future.

APPENDIX A: FREQUENCY-DOMAIN RESULTS

In this Appendix we show how the basic result (8) can alternatively be used to relate the output spectrum to the input spectrum of a two-photon wave packet, which allows for an easier comparison to some previous works.

Beginning with the unidirectional case, the double Fourier transform of Eq. (16) (suitably symmetrized) yields the final spectrum

$$\tilde{f}_{\rm uni}(\omega_1,\omega_2) = \tilde{f}_0(\omega_1,\omega_2) - 2\Gamma\left[\frac{\tilde{f}_0(\omega_1,\omega_2)}{\Gamma - i\omega_1} + \frac{\tilde{f}_0(\omega_1,\omega_2)}{\Gamma - i\omega_2}\right] + \frac{4\Gamma^2\,\tilde{f}_0(\omega_1,\omega_2)}{(\Gamma - i\omega_1)(\Gamma - i\omega_2)} - \frac{2\Gamma^2}{\pi}\left[\frac{1}{\Gamma - i\omega_1} + \frac{1}{\Gamma - i\omega_2}\right]\int \frac{d\omega'\,\tilde{f}_0(\omega',\omega_1+\omega_2-\omega')}{(\Gamma - i\omega')(\Gamma - i(\omega_1+\omega_2-\omega'))} \tag{A1}$$

in terms of the original spectrum $\tilde{f}_0(\omega_1,\omega_2)$. Anticipating the bidirectional case, we define transmission and reflection coefficients t_ω and r_ω as

$$t_\omega = \frac{i\omega}{\Gamma - i\omega} \tag{A2}$$

$$r_\omega = \frac{\Gamma}{\Gamma - i\omega} \tag{A3}$$

in terms of which the above result takes the more compact form

$$\tilde{f}_{\rm uni}(\omega_1,\omega_2) = \tilde{f}_0(\omega_1,\omega_2)(r_{\omega_1}+t_{\omega_1})(r_{\omega_2}+t_{\omega_2}) - \frac{2\Gamma^2}{\pi}\left[\frac{1}{\Gamma-i\omega_1}+\frac{1}{\Gamma-i\omega_2}\right] \times \int \frac{d\omega'\,\tilde{f}_0(\omega',\omega_1+\omega_2-\omega')}{(\Gamma-i\omega')(\Gamma-i(\omega_1+\omega_2-\omega')}. \quad \text{(A4)}$$

This is a general result, valid for an arbitrary initial state. For an initially separable state [$\tilde{f}_0(\omega_a,\omega_b)=\tilde{f}_0(\omega_a)\tilde{f}_0(\omega_b)$] where the two photons are identical the last term in (A4) can be expressed as a convolution:

$$\tilde{f}_{\rm uni}(\omega_1,\omega_2) = \tilde{f}_0(\omega_1)\tilde{f}_0(\omega_2)(r_{\omega_1}+t_{\omega_1})(r_{\omega_2}+t_{\omega_2}) - \frac{2\Gamma^2}{\pi}\left[\frac{1}{\Gamma-i\omega_1}+\frac{1}{\Gamma-i\omega_2}\right] \times \left[\left(\frac{\tilde{f}_0(\omega_1+\omega_2)}{(\Gamma-i(\omega_1+\omega_2))}\right) * \left(\frac{\tilde{f}_0(\omega_1+\omega_2)}{(\Gamma-i(\omega_1+\omega_2))}\right)\right], \quad \text{(A5)}$$

where the * represents the convolution between the functions within the parentheses. The notation in Eq. (A5) is meant to suggest that the result of the (one-dimensional) convolution is a function of $\omega_1+\omega_2$, as shown in Eq. (A4). This convolution term is the bound or entangled component of the state, in the frequency domain.

For the bidirectional case, initial state $|2,0\rangle$, the Fourier transform of Eqs. (30) yields

$$\tilde{f}_{a_{2,0}}(\omega_1,\omega_2) = t_{\omega_1}t_{\omega_2}\tilde{f}_0(\omega_1)\tilde{f}_0(\omega_2)+\frac{1}{4}\tilde{f}_{\rm ent}(\omega_1,\omega_2)$$

$$\tilde{f}_{b_{2,0}}(\omega_1,\omega_2) = r_{\omega_1}r_{\omega_2}\tilde{f}_0(\omega_1)\tilde{f}_0(\omega_2)+\frac{1}{4}\tilde{f}_{\rm ent}(\omega_1,\omega_2)$$

$$\tilde{f}_{{\rm split}_{2,0}}(\omega_1,\omega_2) = \sqrt{2}\,t_{\omega_1}r_{\omega_2}\tilde{f}_0(\omega_1)\tilde{f}_0(\omega_2)+\frac{\sqrt{2}}{4}\tilde{f}_{\rm ent}(\omega_1,\omega_2). \quad \text{(A6)}$$

Note that they only differ by the factors in front of the first term and that when $\Gamma=0$ they reduce to a two-photon pulse traveling to the right. The transmission and reflection coefficients also correspond to the different processes occurring. For example, $\tilde{f}_{b_{2,0}}$ represents two photons being transmitted through the atom while $\tilde{f}_{{\rm split}_{2,0}}$ represents one photon being reflected and the other being transmitted. These equations have exactly the same form as Eq. (22) in Ref. [2].

For the Gaussian wave packet defined by Eq. (31) the entangled component of the spectrum is given by

$$\tilde{f}_{\rm ent} = -\frac{4\Gamma^2 T\sqrt{\frac{2}{\pi}}}{(\Gamma-i\omega_1)(\Gamma-i\omega_2)}e^{-((1+i)\Gamma+\omega_1+\omega_2)((-1+i)\Gamma+\omega_1+\omega_2)T^2} \times {\rm erfc}\left[\frac{T}{\sqrt{2}}[2\Gamma-i(\omega_1+\omega_2)]\right]. \quad \text{(A7)}$$

For the flat-top pulse the entangled component is much more complicated than for the Gaussian, but it may still be computed analytically, with the result

$$\tilde{f}_{\rm bound}(\omega_1,\omega_2) = \frac{2\Gamma e^{-(\omega_1+\omega_2)(2i\Gamma+\omega_1+\omega_2-4ia^2t_0)/4a^2}}{\pi\mathcal{N}(\Gamma-i\omega_1)(\Gamma-i\omega_2)(\Gamma-i(\omega_1+\omega_2))}\left\{e^{\Gamma^2/2a^2}\left[(1+e^{i\mathcal{T}(\omega_1+\omega_2)})\,{\rm erfc}\left(\frac{2\Gamma-i(\omega_1+\omega_2)}{2\sqrt{2}a}\right)\right.\right. - e^{\Gamma\mathcal{T}}{\rm erfc}\left(\frac{2a^2\mathcal{T}+2\Gamma-i(\omega_1+\omega_2)}{2\sqrt{2}a}\right)+e^{-\Gamma\mathcal{T}+i\mathcal{T}(\omega_1+\omega_2)}\left({\rm erfc}\left(\frac{2a^2\mathcal{T}-2\Gamma+i(\omega_1+\omega_2)}{2\sqrt{2}a}\right)-2\right)\Big] - \frac{(2i\Gamma+\omega_1+\omega_2)e^{i\Gamma(\omega_1+\omega_2)/2a^2}}{\omega_1+\omega_2}\left[{\rm erf}\left(\frac{2a^2\mathcal{T}-i(\omega_1+\omega_2)}{2\sqrt{2}a}\right)\right. - e^{i\mathcal{T}(\omega_1+\omega_2)}{\rm erf}\left(\frac{2a^2\mathcal{T}+i(\omega_1+\omega_2)}{2\sqrt{2}a}\right)+i\left(1+e^{i\mathcal{T}(\omega_1+\omega_2)}\right){\rm erfi}\left(\frac{\omega_1+\omega_2}{2\sqrt{2}a}\right)\Big]\Big\}. \quad \text{(A8)}$$

For two pulses coming from opposite directions, we find

$$\tilde{f}_{a_{1,1}}(\omega_1,\omega_2)=\tilde{f}_{b_{1,1}}(\omega_1,\omega_2)=\frac{1}{\sqrt{2}}\left((r_{\omega_1}t_{\omega_2}+r_{\omega_2}t_{\omega_1})\tilde{f}_0(\omega_1)\tilde{f}_0(\omega_2)+\frac{1}{2}\tilde{f}_{\rm ent}(\omega_1,\omega_2)\right) \quad \text{(A9)}$$

$$\tilde{f}_{{\rm split}_{1,1}}(\omega_1,\omega_2)=(r_{\omega_1}r_{\omega_2}+t_{\omega_2}t_{\omega_1})\tilde{f}_0(\omega_1)\tilde{f}_0(\omega_2)+\frac{1}{2}\tilde{f}_{\rm ent}(\omega_1,\omega_2). \quad \text{(A10)}$$

APPENDIX B: SOME OBSERVATIONS ON THE UNIDIRECTIONAL CASE

As shown in Sec. III, the two-sided waveguide requires two sets of modes for its description: although things can be arranged so that the atom only interacts with one of the sets (standing waves with the appropriate symmetry), the initial state typically has components on both sets. This is in contrast to the formally simpler unidirectional formalism in Sec. II, which involves only one set of modes.

Although the unidirectional case may seem unrealistic, there are, in fact, schemes that allow one to excite only the set of modes that the atom interacts with. These may be said to realize a unidirectional waveguide, by which we mean one that has effectively only one output port for a given input port. The simplest such scheme is shown in Fig. 13(a). The optical paths can be arranged so that an incoming field along port $a_{\rm in}$ of the beam splitter sets up a standing wave in the guide with the right symmetry to couple maximally to the atom; for instance, for a traveling wave entering from the $a_{\rm in}$ direction, one could

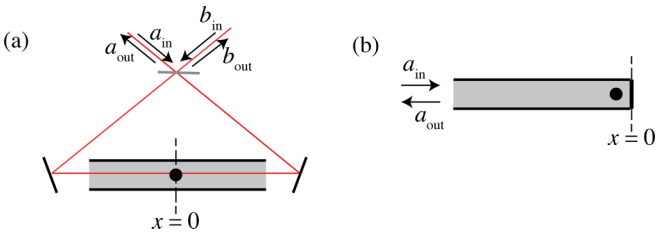

FIG. 13. Two ways to realize the unidirectional waveguide interaction

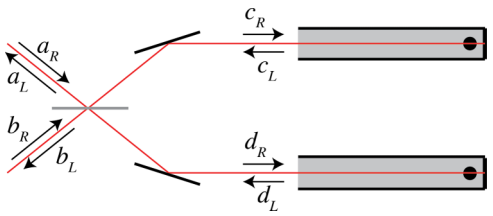

FIG. 14. The scheme to discriminate between one- and two-photon states of Witthaut *et al.* [13].

get a standing wave of the form, say, $\cos(kx)$, whereas for a wave coming from the $b_{\rm in}$ direction, one would get $\sin(kx)$. An atom placed at $x = 0$ would interact only with the first field, and the (bidirectional) field it would emit into such a standing wave mode would recombine at the beam splitter with the right phase to leave entirely along the backwards path $a_{\rm out}$. Of course, at some point along the a path one would need to place a nonreciprocal device, such as a Faraday rotator, to separate the input from the output field. When this is done, however, one would find the output field would have a (running-wave) spectrum related to the input one by the simple unidirectional solutions of Sec. II.

A somewhat less obvious arrangement is provided by the truncated waveguide (with a reflective end) of Fig. 13(b). Its natural modes form a single set of standing waves of the form $\sin(kx)$ (if the reflective end is at $x = 0$). Nonetheless, an incoming field whose spectrum can be expanded on traveling waves of the form e^{ikx}, with $k \sim k_0$, would have a very similar spectrum (except for an overall phase factor) when expanded on the basis of the functions $\sin(kx) = (e^{ikx} - e^{-ikx})/2i$, since the e^{-ikx} part would not be expected to make a large contribution, provided k_0 is large enough (the precise condition is that $\omega_0 T \gg 1$, where $\omega_0 = ck_0$, and T is the pulse duration; this is essentially the rotating-wave approximation).

Next, the atom must be placed at a location x_0 such that $|\Delta k\, x_0| \ll 1$, to ensure it couples to all the relevant standing waves with approximately the same strength. Here $\Delta k = \Delta\omega/c$ is the pulse's wave-vector spread, of the order of $1/cT$, so the condition is really that $|x_0| \ll cT$, that is, the atom should much closer to the end wall than the width of the pulse.

Finally, after the interaction is over, the field leaving the waveguide will again have an expansion on traveling waves essentially identical to the expansion on the standing waves $\sin(kx) = (e^{ikx} - e^{-ikx})/2i$, where now it is the first (right-traveling) exponential that does not contribute.

Under these conditions, one can basically take the incoming traveling-wave spectrum as the input to the unidirectional formulas of Sec. II, and interpret the output again as a traveling-wave spectrum in the opposite direction. For an initial two-photon state, this final result is given by Eq. (A4).

An interesting application of these unidirectional formulas was recently given by Witthaut, Lukin, and Sørensen in Ref. [13]. Suppose one has two unidirectional waveguides fed through a beam splitter as in Fig. 14. The beam splitter relates the right-traveling modes according to $a_R = (c_R + d_R)/\sqrt{2}$ and $b_R = (c_R - d_R)/\sqrt{2}$; interaction with the atom in the waveguide ultimately leads to replacing the c and d input spectra by the corresponding output spectra, and the c_R and d_R operators by the left-traveling $c_L = (a_L + b_L)/\sqrt{2}$ and $d_L = (a_L - b_L)/\sqrt{2}$. Hence, a single-photon pulse entering from the a_R direction is converted according to

$$\int d\omega\, \tilde{f}_0(\omega) a_{R\omega}^\dagger |0\rangle \to -\int d\omega\, (r_\omega + t_\omega)\, \tilde{f}_0(\omega) a_{L\omega}^\dagger |0\rangle \quad \text{(B1)}$$

(in terms of the coefficients r_ω and t_ω defined in Appendix A), whereas a two-photon pulse undergoes the sequence

$$\begin{aligned} |\psi\rangle = \frac{1}{2\sqrt{2}} \int d\omega_1 d\omega_2\, \tilde{f}_0(\omega_1,\omega_2)(c_{\omega_1}^\dagger c_{\omega_2}^\dagger + d_{\omega_1}^\dagger d_{\omega_2}^\dagger + c_{\omega_1}^\dagger d_{\omega_2}^\dagger \\ + c_{\omega_2}^\dagger d_{\omega_1}^\dagger)_R |0\rangle \to \frac{1}{2\sqrt{2}} \int d\omega_1 d\omega_2 \\ \times [\tilde{f}_{\rm uni}(\omega_1,\omega_2)(c_{\omega_1}^\dagger c_{\omega_2}^\dagger + d_{\omega_1}^\dagger d_{\omega_2}^\dagger)_L \\ + (r_{\omega_1} + t_{\omega_1})(r_{\omega_2} + t_{\omega_2})\, \tilde{f}_0(\omega_1,\omega_2)(c_{\omega_1}^\dagger d_{\omega_2}^\dagger + c_{\omega_2}^\dagger d_{\omega_1}^\dagger)_L]|0\rangle \end{aligned} \quad \text{(B2)}$$

after transforming separately the two terms that represent two-photon interactions with the atom, and the two terms that represent the photons going into separate waveguides and interacting once with each atom. In terms of the final a_L and b_L operators, and using Eq. (A4), this becomes

$$\begin{aligned} |\psi_{\rm out}\rangle = \frac{1}{\sqrt{2}} \int d\omega_1 d\omega_2 \Big[\Big(\tilde{f}_0(\omega_1,\omega_2)(r_{\omega_1} + t_{\omega_1})(r_{\omega_2} + t_{\omega_2}) \\ + \frac{1}{2} \tilde{f}_{\rm ent}(\omega_1,\omega_2) \Big) a_{L\omega_1}^\dagger a_{L\omega_2}^\dagger + \frac{1}{2} \tilde{f}_{\rm ent}(\omega_1,\omega_2) b_{L\omega_1}^\dagger b_{L\omega_2}^\dagger \Big] |0\rangle. \end{aligned} \quad \text{(B3)}$$

As Witthaut *et al.* point out [13], this is an interesting result, in that the two-photon state (B3) has a significant probability to come out through the b port, whereas the one-photon state (B1) always comes out through the a port. Note that the b port output consists exclusively of (part of) the entangled state $f_{\rm ent}$, which also makes it clear that this is a genuine two-photon effect (in interferometric terms, it may be understood as resulting from a nonlinear phase shift). Also, as Eq. (A4) shows, the two terms appearing in the output of the a port have predominantly opposite signs, so it is possible to arrange their partial cancellation, which leads Witthaut *et al.* to suggest that this could be turned into a near-perfect discriminator between one- and two-photon states, by taking the output of port a and feeding it into another, similar arrangement. After a few iterations, they find a large probability that the two-photon

state may have exited through one of the b ports, whereas the single-photon state must still be in the last remaining a port.

It is clear from the explicit expression (20) (as well as, for instance, Fig. 6), that the entangled two-photon wave function can be very different from that of the initial state for large coupling, when (in the space-time domain) its width along a $\tau + \tau' = \text{const}$ line is determined by $1/\Gamma$. Hence, for the partial cancellation in (B3) to work, one would require Γ to be of the order of the pulse's initial spectral width. For a Gaussian pulse, the optimum condition is about $\Gamma T = 0.7$.

The authors of Ref. [13] did not address explicitly the way in which the output state would change after each iteration in their scheme. For the single-photon input, clearly, after n iterations, the output of the final a port would have a spectrum

$$\left(\frac{\Gamma + i\omega}{\Gamma - i\omega}\right)^n \tilde{f}_0(\omega). \tag{B4}$$

For a two-photon input, on the other hand, if we define

$$\Omega(\omega_1,\omega_2) = -\frac{2\Gamma^2}{\pi}\left(\frac{1}{\Gamma - i\omega_1} + \frac{1}{\Gamma - i\omega_2}\right) \tag{B5}$$

$$RT(\omega_1,\omega_2) = (r_{\omega_1} + t_{\omega_1})(r_{\omega_2} + t_{\omega_2}) \tag{B6}$$

$$\text{Int}[\tilde{f}(\omega_1,\omega_2)] = \int \frac{d\omega' \tilde{f}(\omega',\omega_1 + \omega_2 - \omega')}{(\Gamma - i\omega')[\Gamma - i(\omega_1 + \omega_2 - \omega')]} \tag{B7}$$

so that $f_{\text{ent}}(\omega_1,\omega_2) = \Omega(\omega_1,\omega_2)\text{Int}[\tilde{f}(\omega_1,\omega_2)]$, we find that after the pulse is fed through n photon sorters, the remaining component in the last a mode is given by

$$\tilde{f}_{a_n}(\omega_1,\omega_2) = \tilde{f}_{a_{n-1}}(\omega_1,\omega_2)RT(\omega_1,\omega_2) + \frac{1}{2}\Omega(\omega_1,\omega_2)\text{Int}[\tilde{f}_{a_{n-1}}(\omega_1,\omega_2)]. \tag{B8}$$

Consider the case in which the initial pulse is in a separable state of the form $\tilde{f}_0(\omega_1)\tilde{f}_0(\omega_2)$. After the first pass, $\text{Int}[\tilde{f}(\omega_1)\tilde{f}(\omega_2)] = \tilde{G}(\omega_1 + \omega_2) * \tilde{G}(\omega_1 + \omega_2)$. One can see that this term will not be modified by any future integrals, since, when we apply the Int operator, we let $\omega_1 \to \omega_a$ and $\omega_2 \to \omega_1 + \omega + 2 - \omega_a$. With this transformation any function of $\omega_1 + \omega_2$ has no dependence on ω_a. This property also applies to functions containing RT and Ω as well. Using this, it becomes possible to evaluate the total expression for each pass by hand. After a few passes one finds a pattern that can be expressed as

$$\tilde{f}_{a_n}(\omega_1,\omega_2) = \tilde{f}(\omega_1)\tilde{f}(\omega_2)RT^n(\omega_1,\omega_2) + \frac{1}{2}\Omega(\omega_1,\omega_2) \times \sum_{i=0}^{n-1} M_{n-1-i}(\omega_1,\omega_2)\text{Int}[\tilde{f}(\omega_1)\tilde{f}(\omega_2)RT^i(\omega_1,\omega_2)] \tag{B9}$$

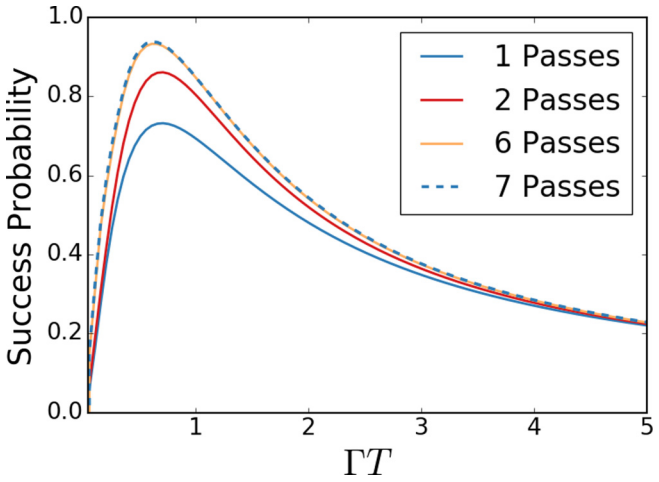

FIG. 15. The success probability as a function of ΓT for up to seven passes through the photon sorter. Note the 6 and 7 cases are already virtually indistinguishable.

with each $M_n(\omega_1,\omega_2)$ given by

$$M_n(\omega_1,\omega_2) = RT^n(\omega_1,\omega_2) + \sum_{j=1}^{n} M_{j-1}(\omega_1,\omega_2) \times \text{Int}\left[\frac{\Omega(\omega_1,\omega_2)}{2}RT^{n-j}(\omega_1,\omega_2)\right]. \tag{B10}$$

Unfortunately, the term $\text{Int}[\tilde{f}(\omega_1)\tilde{f}(\omega_2)RT^m(\omega_1,\omega_2)]$ in Eq. (B9) prevents a completely analytic solution even for a Gaussian pulse; however, the recursive solution for M_n lends itself to a computational approach. By calculating each M_n and $\text{Int}[\tilde{f}(\omega_1)\tilde{f}(\omega_2)RT^m(\omega_1,\omega_2)]$ and saving the samples of the functions as arrays we can efficiently calculate the successful discrimination probability for a large number of passes. This is given by

$$P_{\text{success}} = 1 - \int d\omega_1 d\omega_2 |\tilde{f}_{a_n}(\omega_1,\omega_2)|^2 \tag{B11}$$

and is shown in Fig. 15 below.

As can be seen in Fig. 15 the success probability peaks for relatively low values of Γ. For one pass the success probability reaches a maximum of 0.732 when $\Gamma = 0.704$. Continuing this for multiple passes, one finds that as the number of photon sorters increases the benefit of adding more sorters decreases very quickly. For $\Gamma = 0.704$ after 100 passes through the device the success probability is 0.940, which is merely a 0.34% increase from 10 passes.

We note that this result is in slight disagreement with the claim in Ref. [13] that the success probability could be as high as 0.96 with only five sorters. At present we do not know the reason for this discrepancy.

[1] J. T. Shen and S. Fan, Phys. Rev. Lett. **98**, 153003 (2007).
[2] H. Zheng, D. J. Gauthier, and H. U. Baranger, Phys. Rev. A **82**, 063816 (2010).
[3] E. E. Hach, III, A. W. Elshaari, and S. F. Preble, Phys. Rev. A **82**, 063839 (2010).
[4] S. Fan, S. E. Kocabas, and J. T. Shen, Phys. Rev. A **82**, 063821 (2010).

[5] M. P. Schneider, T. Sproll, C. Stawiarski, P. Schmitteckert, and K. Busch, Phys. Rev. A **93**, 013828 (2016).
[6] B. Q. Baragiola, R. L. Cook, A. M. Brańczyk, and J. Combes, Phys. Rev. A **86**, 013811 (2012).
[7] Y. Wang, J. Minar, and V. Scarani, Phys. Rev. A **86**, 023811 (2012).
[8] A. Roulet, H. N. Le, and V. Scarani, Phys. Rev. A **93**, 033838 (2016).
[9] K. Kojima, H. F. Hofmann, S. Takeuchi, and K. Sasaki, Phys. Rev. A **68**, 013803 (2003).
[10] S. Derouault and M. A. Bouchene, Phys. Lett. A **376**, 3491 (2012).
[11] Y. Chen, M. Wubs, J. Mørk, and A. F. Koenderink, New J. Phys. **13**, 103010 (2011).
[12] A. Nysteen, P. T. Kristensen, D. P. S. McCutcheon, P. Kaer, and J. Mørk, New J. Phys. **17**, 023030 (2015).
[13] D. Witthaut, M. D. Lukin, and A. S. Sørensen, Europhys. Lett. **97**, 50007 (2012).
[14] J. Gea-Banacloche, Phys. Rev. A **87**, 023832 (2013).
[15] See, for example, M. O. Scully and M. S. Zubairy, *Quantum Optics*, Section 4.2 (Cambridge University Press, Cambridge, 1997).
[16] P. L. Kelley and W. H. Kleiner, Phys. Rev. **136**, A316 (1964).
[17] I. H. Deutsch, R. Y. Chiao, and J. C. Garrison, Phys. Rev. Lett. **69**, 3627 (1992).
[18] Z. Cheng and G. Kurizki, Phys. Rev. Lett. **75**, 3430 (1995).
[19] D. E. Chang, A. S. Sørensen, E. A. Demler, and M. D. Lukin, Nat. Phys. **3**, 807 (2007).
[20] O. Firstenberg, T. Peyronel, Q.-Y. Liang, A. V. Gorshkov, M. D. Lukin, and V. Vuletić, Nature (London) **502**, 71 (2013).
[21] J. D. Franson, Phys. Rev. Lett. **62**, 2205 (1989).
[22] A. Einstein, B. Podolsky, and N. Rosen, Phys. Rev. **47**, 777 (1935).
[23] Examples of this sort of transient solutions may be found, for instance, in Ref. [12].
[24] This is essentially the same as Eq. (12) of Ref. [11], the only difference being that in that paper the initial condition was that the atom be in the ground state at $t = 0$, whereas we have assumed it to be in the ground state at $t = -\infty$, that is, well before the arrival of the pulse.
[25] For the Gaussian pulse, these results were first presented (to our knowledge) in Ref. [2]. They can also be seen in Fig. 5(b) of Ref. [12], only there they are plotted versus the spectral, rather than the temporal, width of the pulse.
[26] We also plot the results as functions of $\tau = t \pm z/c$, rather than t or z, so our figures are always centered at the position of an (imaginary) undisturbed transmitted or specularly reflected pulse. A different approach can be seen in Ref. [12], where the (numerically calculated) probability densities have been plotted as functions of z_1 and z_2, so each figure includes all three possible outcomes, and shows the spatial propagation as well. Compare, in particular (as the example where their parameters seem to be closest to some of ours), the rightmost figure in the top row of Fig. 3 of Ref. [12] to a combination of our Figs. 6(g), 6(h), and 6(i).
[27] C. K. Hong, Z. Y. Ou, and L. Mandel, Phys. Rev. Lett. **59**, 2044 (1987).